

THE ROLE OF TETRACYCLINE AND MACROMOLECULAR CROWDING ON  
THE FUNCTION OF ELONGATION FACTOR-TU

**KATHERINE ELIZABETH GZYL**  
**Bachelor of Science, University of Lethbridge, 2013**

A Thesis/Project  
Submitted to the School of Graduate Studies  
of the University of Lethbridge  
in Partial Fulfillment of the  
Requirements for the Degree

**MASTER OF SCIENCE**

Chemistry and Biochemistry  
University of Lethbridge  
LETHBRIDGE, ALBERTA, CANADA

© Katherine Elizabeth Gzyl, 2017

THE ROLE OF TETRACYCLINE AND MACROMOLECULE CROWDING ON THE  
FUNCTION OF ELONGATION FACTOR-TU

KATHERINE ELIZABETH GZYL

Date of Defence: April 21, 2017

Dr. H.-J. Wieden Supervisor	Professor	Ph.D.
--------------------------------	-----------	-------

Dr. U. Kothe Thesis Examination Committee Member	Associate Professor	Ph.D.
---	---------------------	-------

Dr. M. Roussel Thesis Examination Committee Member	Professor	Ph.D.
---	-----------	-------

Dr. S. McKenna External Examiner University of Manitoba Winnipeg, Manitoba	Associate Professor	Ph.D.
---	---------------------	-------

Dr. M. Gerken Chair, Thesis Examination Committee	Professor	Ph.D.
--	-----------	-------

## **Dedication**

Dedicated to,

My parents who have always given me endless support and encouragement.

My brother for always being there and putting up with all my science talk.

My husband who willingly read, listened, and was interested in my work. And gave me encouragement, support and love when I needed it most.

## **Abstract**

The cellular environment affects dynamics of proteins moving from one conformation into another. Aspects of the cellular environment such as availability of ligands, osmolytes, and antibiotics affect proteins. However, the effect of macromolecular crowding remains debated. The translational GTPase EF-Tu undergoes a large conformational change during its delivery of aa-tRNA to the ribosome. Here, we investigated whether the antibiotic tetracycline or the crowded nature of the cell has an affect on the dynamics of EF-Tu. By comparing the rates of nucleotide binding, the GTPase activity of EF-Tu, and the stability of the EF-Tu•GTP•aa-tRNA complex with and without tetracycline, it was concluded that tetracycline did not affect the function of EF-Tu. Macromolecular crowding by the synthetic crowding agents dextran 40 and PEG 4000 was found to influence the dynamics of nucleotide binding in EF-Tu suggesting the dynamics and function of EF-Tu should be studied in a more cellular-like context.

## **Acknowledgements**

I would like to thank my thesis supervisor Dr. Hans-Joachim Wieden for giving me the opportunity to study what I enjoy and am passionate about. Dr. Hans-Joachim Wieden provided me with the guidance, critical feedback, and patience I needed to complete my MSc.

I would like to thank the members of my supervisory committee, Dr. Marc Roussel and Dr. Ute Kothe, for their critical feedback and encouragement.

I would like to thank all the members I have worked with in the Wieden and Kothe Labs for their feedback, encouragement and friendship.

I would especially like to thank Isadora Fantacini Masiero for performing some of the nucleotide dissociation time courses in the presence of tetracycline, Emily Wilton for her help editing the tetracycline transcript, and Dylan Girodat for performing the molecular dynamics simulations and determining and plotting the root mean square flexibility (RMSF) of EF-Tu in the GTP and GDP state.

## Table of Contents

List of Tables.....	vii
List of Figures.....	viii
List of Abbreviations.....	ix
Chapter 1: Introduction.....	1
Chapter 2: Tetracycline does not directly affect EF-Tu function.....	17
Chapter 3: Macromolecular crowding affects the nucleotide binding properties of elongation factor-Tu.....	51
Chapter 4: Conclusion.....	79

## List of Tables

Table 1: Kinetic parameters of nucleotide binding in EF-Tu in the presence of 0 $\mu\text{M}$ and 100 $\mu\text{M}$ tetracycline. ....	35
Table 2: Effect of 100 $\mu\text{M}$ tetracycline on the intrinsic, 70S-, and 50S-stimulated GTPase activity of EF-Tu. ....	44
Table 3: Effect of tetracycline on the ability of EF-Tu to protect the amino-ester bond in Phe-tRNA <sup>Phe</sup> . ....	49
Table 4: Regions in the GTP and GDP conformation of EF-Tu that are more flexible compared to the entire structure during 40 ns molecular dynamics simulations. These are the same regions that are flexible in Figures 22 and Figure 23. ....	73

## List of Figures

Figure 1: Domain arrangement of EF-Tu in the GTP and GDP conformation.....	4
Figure 2: Bacterial translation.....	5
Figure 3: Model of the EF-Tu•GTP•aa-tRNA complex. ....	6
Figure 4: Primary binding site of tetracycline on the 30S ribosomal subunit.....	9
Figure 5: Binding pocket of tetracycline in EF-Tu. ....	11
Figure 6: Tetracycline binds proximal to switch I and II in EF-Tu. ....	21
Figure 7: Tetracycline binding is compatible with EF-Ts binding to EF-Tu.....	22
Figure 8: Fluorescence emission properties of tetracycline and mant-nucleotides. ....	24
Figure 9: Effect of tetracycline on the association rate of EF-Tu and mant-nucleotides...	32
Figure 10: Kinetic mechanism of nucleotide exchange in EF-Tu. ....	33
Figure 11: Effect of tetracycline on the dissociation rate of EF-Tu and mant-nucleotides. ....	37
Figure 12: Effect of tetracycline on EF-Ts-stimulated dissociation of mant-nucleotides from EF-Tu. ....	40
Figure 13: Effect of tetracycline on the intrinsic GTPase activity.....	43
Figure 14: Ribosome-stimulated GTPase activity. ....	46
Figure 15: Effect of tetracycline on aminoacyl-tRNA protection by EF-Tu. ....	48
Figure 16: Effect of molecular crowding on the association rate of GTP. ....	60
Figure 17: Effect of molecular crowding on the association rate of GTP. ....	61
Figure 18: Effect of molecular crowding on the association rate of GDP.....	63
Figure 19: Effect of molecular crowding on the association rate of GDP.....	64
Figure 20: Effect of macromolecular crowding on the dissociation rate of GTP.....	67
Figure 21: Effect of macromolecular crowding on the dissociation rate of GDP.....	68
Figure 22: Cartoon representation of EF-Tu in the GTP and GDP bound states.....	71
Figure 23: RMSF with respect to the C <sub>α</sub> of each amino acid for 40 ns MD simulations. .	72



## List of Abbreviations

Aminoacyl -transfer RNA	aa-tRNA
Elongation factor-thermal stable	EF-Ts
Elongation factor thermal unstable	EF-Tu
EF-Tu•GTP•aa-tRNA ternary complex	TC
Eukaryotic initiation factor 4A	eIF4A
Fluorescent resident energy transfer	FRET
Guanine nucleotide exchange factor	GEF
Guanosine-5'-diphosphate	GDP
Guanosine-5'-triphosphate	GTP
Inorganic phosphate	P <sub>i</sub>
Minimal inhibitory concentration	MIC
Molecular dynamics	MD
(Poly)ethylene glycol	PEG
Ribosomal RNA	rRNA
Root mean square fluctuation	RMSF

## **Chapter 1: Introduction**

### **Role of the cellular environment on protein dynamics**

Proteins adopt specific conformations to perform their functions in the cell. Different populations of conformations are controlled by factors in the cellular environment such as the availability of ligands (1), the presence of small molecule inhibitors (2, 3), the presence of osmolytes (4), and the crowded matrix of the cell (5). For instance, the concentration of GTP in the cell is about 10-fold greater than the GDP concentration in exponentially growing *Escherichia coli* (1). This concentration difference contributes to the binding of GTP over GDP to guanine binding proteins; therefore, favoring the GTP-bound over the GDP-bound conformation (6). Small molecule inhibitors, such as antibiotics, can trap a protein in an inactive conformation and prevent it from functioning (2, 3). Osmolytes such as glucose and sucrose are known to stabilize protein conformations (7). Macromolecular crowding is a phenomenon present in all cells (8); albeit, it is unknown how the densely packed environment of the cell influences the conformation or function of proteins. Here, two questions regarding the relationship between protein dynamics and function were addressed. First, the poorly understood effect of the antibiotic tetracycline on the function of the GTPase Elongation factor (EF)-Tu was investigated. Secondly, the effect that molecular crowding has on the nucleotide-binding properties of EF-Tu was studied.

### **Role of elongation factor Tu in bacterial translation**

EF-Tu is a universally conserved bacterial protein that belongs to the family of translational GTPases, which have GTPase activity that is activated by the ribosome (9). Like all known GTPase, EF-Tu cycles between an active GTP state and an inactive GDP

conformation. EF-Tu consists of a G domain or domain I, domain II, and domain III that reorient depending on the nucleotide bound (Figure 1). The conformational change from the GTP state to the GDP state involves the conserved switch I and switch II regions found in GTPases (10-12). During the transition from the GTP to GDP bound state, domain I rotates 90° relative to domain II and domain III. This change exposes new surfaces along domain I and domain II (11, 13, 14). The conformation of EF-Tu directs the order by which protein and RNA factors associate to EF-Tu during translation (Figure 2). In the active state, EF-Tu has a high affinity for aminoacyl (aa)-(t)transfer RNA and forms the EF-Tu•GTP•aa-tRNA ternary complex (TC). While the aa-tRNA is part of the TC (figure 3) the aminoacyl-ester bond connecting the amino acid to the tRNA body is protected from spontaneous hydrolysis by ~10 fold (15). The TC associates with the L7/L12 stalk of the 50S subunit, then proceeds to interact with the A site on the 30S subunit of actively translating ribosomes (16, 17). Initial binding of the TC to the ribosome is codon independent; however, the ribosome activates the GTPase activity of EF-Tu when the aa-tRNA anticodon matches the mRNA codon present in the A site (18). The degree of GTPase activation by the ribosome depends on the degree of codon-anticodon complementarity (19). No complementarity results in a biologically insignificant rate of GTP hydrolysis ( $\sim 10^{-2}$  to  $10^{-3}$  s<sup>-1</sup>) (18). Complete complementarity results in a rate of GTPase activation up to 500 s<sup>-1</sup> and a very fast rate of GTP hydrolysis ( $>1000$ s<sup>-1</sup>) (20). EF-Tu alone hydrolyses GTP with a rate ( $\sim 10^{-5}$  to  $10^{-4}$  s<sup>-1</sup>) that is biologically insignificant (21, 22). After GTP hydrolysis and inorganic phosphate (P<sub>i</sub>) release, EF-Tu relaxes from the tight GTP conformation to the relaxed GDP conformation and the affinity for aa-tRNA significantly decreases (23). To complete the GTPase cycle,

EF-Tu associates with its guanine nucleotide exchange factor (GEF) EF-thermal stable (Ts), which accelerates dissociation of guanine nucleotides by ~6000 fold (6). Without EF-Ts, EF-Tu cannot sustain an *in vivo* translation rate. This conformational transition from the GTP to GDP bound state of EF-Tu keeps repeating throughout the elongation phase of translation.

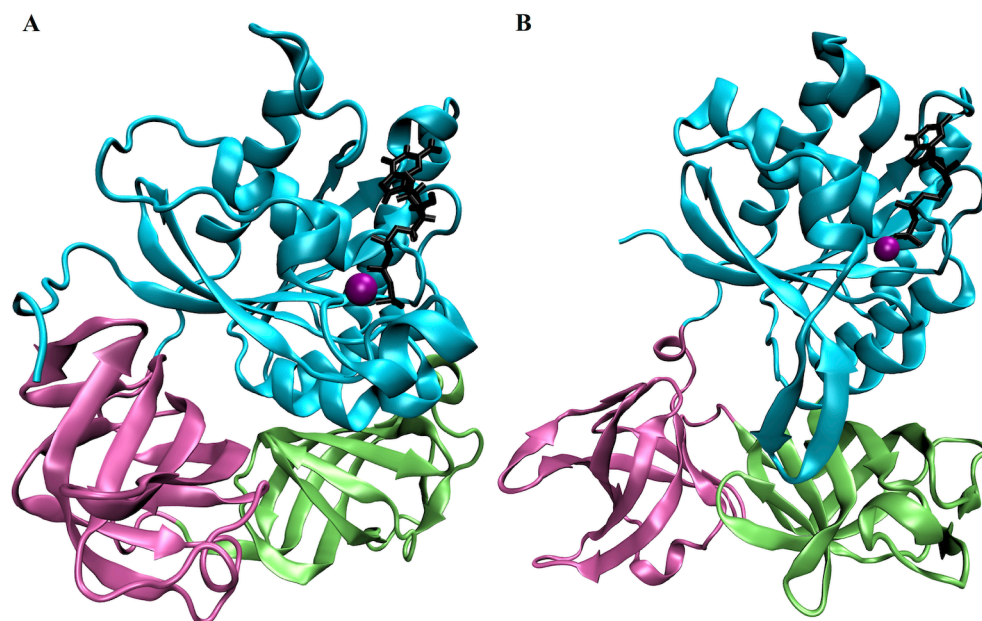


**Figure 1: Domain arrangement of EF-Tu in the GTP and GDP conformation.**

Cartoon illustration of EF-Tu in the GTP state (panel A) and the GDP state (panel B). Domain I is cyan, domain II is pink, domain III is green, the magnesium ion is purple, and the nucleotide is black. Panel (A) is an *E. coli* homology model of the crystal structure of *Thermus aquaticus* EF-Tu•GTP (PDB ID 1EFT) (12), and panel (B) is the EF-Tu•GDP crystal structure (PDB ID 1EFC) (24).

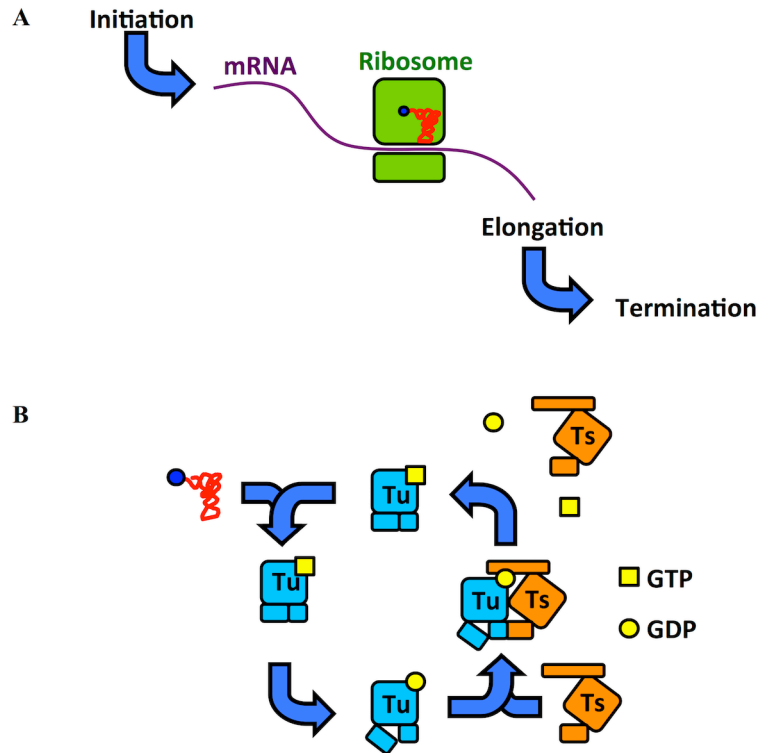


**Figure 2: Bacterial translation.**

Schematic representation of bacterial translation where the ribosome is green, aa-tRNA is red, EF-Tu (Tu) is blue, and EF-Ts (Ts) is orange. (A) The three phases of translation, which are initiation, elongation and termination. (B) The nucleotide exchange cycle of EF-Tu during the elongation phase of translation. During elongation EF-Tu•GTP delivers aa-tRNA to the A site of the ribosome. After a correct codon-anticodon interaction, GTP hydrolysis can occur and EF-Tu can dissociate from the aa-tRNA and ribosome. In order for EF-Tu to participate in another round of translation it is recycled back to the GTP state. Under physiological conditions, EF-Ts catalyzes the dissociation of GDP from EF-Tu in order for a GTP molecule to bind.



**Figure 3: Structure of the EF-Tu•aa-tRNA complex.**

The cartoon representation was based on the crystal structure of the EF-Tu•GTP•aa-tRNA complex (PDB ID 1OB2), and EF-Tu is red and the tRNA is orange.

## **Antibiotics that target elongation factor Tu**

Due to the importance of EF-Tu during bacterial translation, the dynamics of EF-Tu interacting with its different partners and ligands has been the subject of numerous studies. Structural studies including X-ray crystallography and electron microscopy have been used in connection with molecular dynamics simulations and biochemical experiments to investigate the structural dynamics of EF-Tu (25, 26). Small molecule inhibitors have been used to determine how protein dynamics are influenced, so that the protein can no longer perform its function (2, 3, 27, 28). There are a number of antibiotics that interfere with the ability of EF-Tu to deliver the correct aa-tRNA efficiently to the ribosome (28). These antibiotics either act directly on EF-Tu or prevent EF-Tu from associating with the A site of the ribosome (29). To date, EF-Tu is the direct target of four structurally distinct classes of antibiotics that can be divided into two modes of action (28). Kirromycin (2) and enacyloxin IIa (3) both bind to the domain I/III interface and trap EF-Tu in a GTP-like state that prevents the release of EF-Tu•GDP from the ribosome. This results in the accumulation of blocked nonfunctional ribosomes. Pulvomycin and GE2270 A prevent the formation of a stable TC by sterically blocking EF-Tu•GTP from associating with aa-tRNA (27). Pulvomycin binds along the domain I/III interface with its lactone ring binding into the domain II interface, and GE2270 A binds along the domain I/II interface in the GTP conformation of EF-Tu and only interacts with domain I in the GDP conformation of EF-Tu. Kirromycin, enacyloxin IIa, and pulvomycin increase the GTPase activity of EF-Tu (3, 27, 28). The third group of antibiotics that have been suggested to interact with EF-Tu are the tetracyclines (14, 30). However, the effects on the key enzymatic properties of EF-Tu are only poorly described,



and contradicting evidence has been reported in the past (30-32).

The tetracycline family of antibiotics can be separated into typical tetracyclines and atypical tetracyclines. Typical tetracyclines bind to the 30S ribosomal subunit and sterically block aa-tRNA from accommodating in the A site, while atypical tetracyclines target the bacterial cytoplasmic membrane (33). The accepted mode of action of typical tetracyclines is inhibition of cell growth by blocking aa-tRNA accommodation into the A site of the ribosome, which results in a halt of translation (32, 34, 35). Tetracycline binds in the irregular minor groove of helix 34 and the stem loop of helix 31 in the 16S rRNA, as depicted in Figure 4 (34-36). Tetracycline binding relies on interactions with magnesium ions, hydrophobic interactions and stacking interactions, and there are no specific nucleotide or amino acid interactions (37, 38). The unspecific interactions of tetracycline allow it to interact with secondary targets. Biochemical and crystallographic evidence suggests that tetracycline binds to secondary sites on the 30S and 50S subunits (35, 39). Whether these secondary-binding sites contribute to the primary mode of tetracycline action, have an alternative mode of action, or have no effect on translation is not known (35, 40). Additionally, translation inhibition by tetracycline *in vitro* requires concentrations higher than the observed minimal inhibitory concentration (MIC) *in vivo* (36, 41) suggesting aa-tRNA accommodation is not the only target of tetracycline.

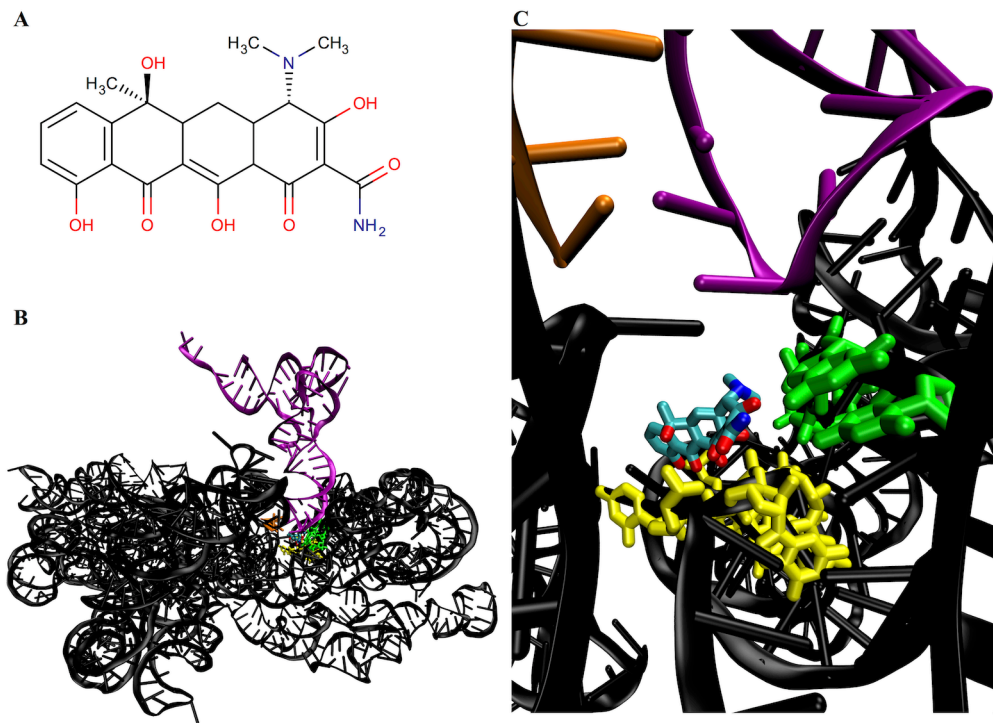


**Figure 4: Primary binding site of tetracycline on the 30S ribosomal subunit.**

Panel (A) shows the structure of tetracycline. Panel (B) illustrates the binding pocket of tetracycline (PDB ID 1HNW), and Panel (C) is a close up of the tetracycline-binding pocket in panel (B) (34). Tetracycline is colored by atom, the irregular minor groove of helix 34 is yellow, the stem loop of helix 31 is green, the remaining 16S-RNA is black, and the fragment of mRNA is orange, the tRNA is purple.

Evidence for the role of EF-Tu as one of tetracycline's secondary targets comes from two crystal structures of a partially trypsin digested EF-Tu•GDP•tetracycline complex (14) (Figure 5). In one case, the trypsin-modified EF-Tu•GDP•tetracycline complex was crystalized, and in the other case, trypsin-modified EF-Tu•GDP was crystalized and tetracycline was soaked into the crystals. In both cases, tetracycline was found to bind to domain I of EF-Tu, having contacts with conserved amino acids in the phosphate binding loop and the switch I region. Based on the interaction with these functionally relevant regions of EF-Tu, it was speculated that tetracycline binding to EF-Tu could have an effect on the structural dynamics of EF-Tu and as a consequence modulate its key enzymatic properties such as guanine nucleotide binding, nucleotide exchange and/or GTP hydrolysis.

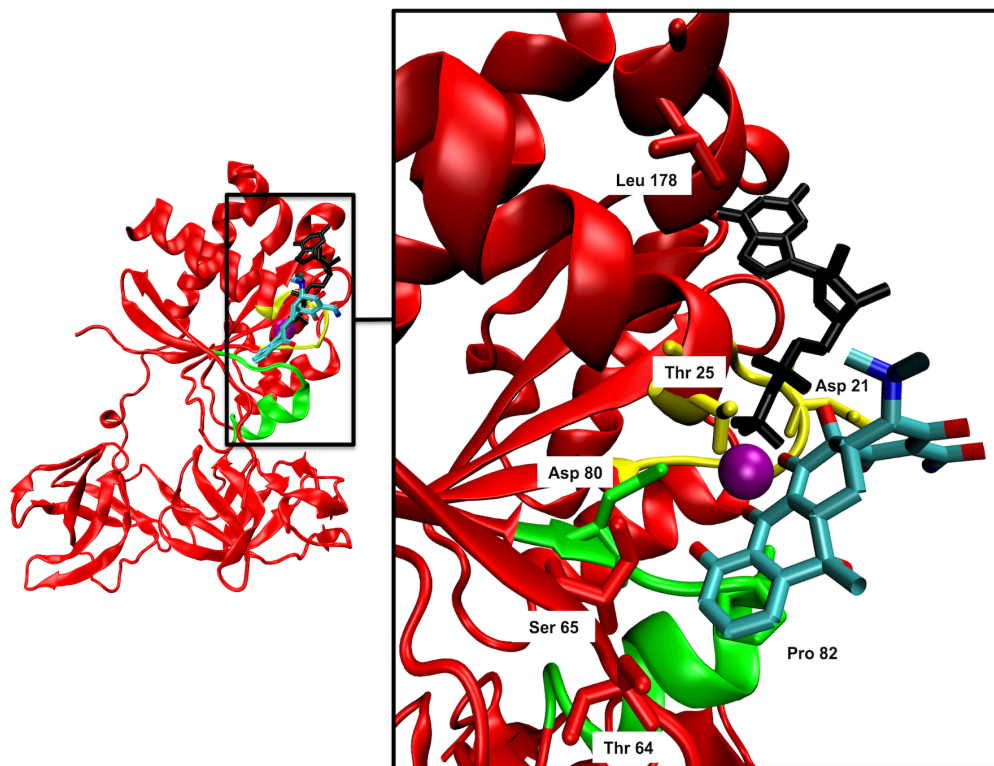


**Figure 5: Binding pocket of tetracycline in EF-Tu.**

The GTPase domain of EF-Tu (red) bound to GDP (black) and tetracycline (colored by atom). Switch II is highlighted in green and the P-loop is highlighted in yellow. Tetracycline is coordinated by the conserved magnesium ion (purple), and interacts with Thr25 (*E. coli* numbering), Asp80, and Pro82, and is in close proximity to Asp21, Thr64, Ser65, and Leu178. The X-ray structure of the EF-Tu•GDP•tetracycline complex (PDB ID 2HCJ) (42) was used to generate the cartoon illustration.

## **Role of macromolecular crowding on protein dynamics**

Over half of all known antibiotics target the processes of translation (29, 43). A great deal of investment has gone into understanding the molecular mechanisms of these antibiotics. However, most of these studies have been performed under *in vitro* conditions that do not represent the crowded environment of the cell. For instance, most proteins are studied at concentrations below 1 g/L (6, 44-46) whereas the cytoplasm of *E. coli* is estimated to contain a concentration between 300 g/L and 400 g/L of protein and RNA (47). Currently, there are no published studies addressing the role of macromolecular crowding on the modes of action of antibiotics. Macromolecular crowding has been shown to alter the activity of small molecule compounds (48). A study focusing on the ability of small molecule inhibitors to interfere with telomere maintenance through the stabilization of the telomere G-quadruplex found that under crowded conditions these ligands had diminished stabilizing ability (48). Before perusing studies that address the effects of antibiotics on the translation process, it should be established whether crowding does alter the process of translation. The only direct evidence that crowding does affect translation comes from the increased activity of the integrated rRNA transcription and ribosome assembly system with the addition of the crowding agent Ficoll 400; however, it is unknown whether Ficoll affects transcription or translation (49). No studies have been conducted on the functions of individual components of the translation machinery under crowded conditions.

It would be ideal to study proteins in a more biologically relevant context such as in cell lysates, but experimentally it is very difficult and often not feasible to use cell lysates in many *in vitro* studies (50). Synthetic polymers such as dextran, ficoll,

(poly)ethylene glycol (PEG) and poly(vinylpyrrolidone) have been used to create crowded conditions *in vitro*. As well natural protein crowders such as bovine serum albumin and lysozyme have been used. The benefit of using synthetic polymers is that they are highly soluble and inert compared to proteins (51). The crowded environment created by either synthetic polymers or natural proteins can result in the macromolecular crowding effects of volume exclusion, confinement and nonspecific interactions between the crowding agents and the probe macromolecule (45, 52). Each macromolecule in the cell excludes volume from other macromolecules, because the macromolecule occupies space that cannot be used by another macromolecule. Excluded volume results from one soluble molecule occupying a volume that can no longer be occupied by another soluble molecule (52). Volume exclusion can lead to confinement, which occurs when crowders create a cavity that the macromolecule cannot escape from (53). Nonspecific interaction can occur when the crowder interacts with the macromolecule under study. These interactions can be stabilizing or destabilizing and depend on the chemical nature of the crowder and macromolecule under study (50, 53). Crowding can result in altered activity of macromolecules by compressing flexible regions (5, 54, 55), creating cavities that the macromolecule cannot escape from (53), and altering the stability of the macromolecule through nonspecific interactions with the crowder (50, 53).

The function of EF-Tu has been thoroughly studied using *in vitro* systems that can be adapted to study the role of molecular crowding on this translational GTPase. The large conformational change of EF-Tu from the GTP to the GDP state (Figure 1) makes it an excellent candidate to study the role of macromolecular crowding on protein dynamics. It is known that macromolecular crowding can compress flexible regions of a

protein to bring together distant subunits (5), but it is unknown how crowding affects the motions from one conformation into another. To decipher the roles of volume exclusion and non-specific interactions between EF-Tu and crowding agents, the chemically distinct polymers dextran 40 and PEG were compared. The effects of macromolecular crowding were also compared to the osmolyte glucose, which stabilizes proteins by preferential burial of the protein backbone (7). Studying the effects of macromolecular crowding on EF-Tu facilitates studies on EF-Tu dynamics under more *in vivo* like conditions that can aid in antibiotic development

### **Objectives**

The two objectives of this thesis were to determine if tetracycline or macromolecular crowding had any effect on the dynamics of EF-Tu that contributed to the factor's function. First, I assessed whether the antibiotic tetracycline had any effect on the intrinsic function of EF-Tu. Based on the location of the tetracycline binding site proximal to the nucleotide binding pocket in EF-Tu, it was predicted that tetracycline could interfere with the binding of GTP or GDP to EF-Tu, the interaction with EF-Ts, intrinsic and ribosome stimulated GTPase activity, and the stability of the EF-Tu•GTP•aa-tRNA complex. The stopped-flow method presented in *Gromadski et al* 2002 (6) was adapted to take into account the auto-fluorescence of tetracycline, so that the kinetics of nucleotide-binding in EF-Tu could be assessed in the presence and absence of tetracycline. Through the use of a bandpass filter in the stopped-flow apparatus, it was determined that tetracycline did not affect either spontaneous nucleotide binding or EF-Ts stimulated nucleotide dissociation. Due to the lack of an effect of tetracycline on the EF-Ts stimulated nucleotide dissociation of EF-Tu, it was concluded that interaction

between EF-Tu and EF-Ts was not affected. EF-Tu's GTPase activity was assessed by monitoring the hydrolysis of [ $\gamma$ - $^{32}$ P<sub>i</sub>]-GTP in the absence or presence of 50S and 70S (stimulated) and including the effect of tetracycline. Under all conditions tested, tetracycline did not affect GTP hydrolysis. The last aspect of the EF-Tu tetracycline interaction studied was the stability of the EF-Tu•GTP•aa-tRNA ternary complex (TC) in the presence and absence of tetracycline. It was determined that tetracycline had no effect on the stability of the TC. It was concluded that tetracycline did not affect dynamics of EF-Tu that contributed to the intrinsic function of the factor.

Second, the stopped-flow technique was used to determine if macromolecular crowding affected the dynamics of spontaneous nucleotide binding in EF-Tu. The effect of macromolecular crowding on the dynamics of EF-Tu was studied by observing the rate of nucleotide association and dissociation. It has been shown that to determine the effect macromolecular crowding on ligand binding both the association and dissociation rate constants must be determined, because both can be affected so that the dissociation constant remains the same (4). Using dextran 40 and PEG 4000 as crowding agents, it was determined that macromolecular crowding decreases the rate constant of GTP association, and GDP dissociation from EF-Tu. However, macromolecular crowding did not affect the association of GDP or dissociation of GTP from EF-Tu. This suggests that macromolecular crowding does affect the dynamics of EF-Tu in a manner that increases the affinity for GDP over GTP. This work paves the way to determine how macromolecular crowding affects the mechanism of antibiotics that target EF-Tu. Currently, all known antibiotics stabilize the GTP state of EF-Tu (27). It would be



interesting to determine if the GTP state of EF-Tu is stabilized in the presence of EF-Tu specific antibiotics under crowded conditions.

## Chapter 2: Tetracycline does not directly affect EF-Tu function\*

### Abstract

Understanding the molecular mechanism of antibiotics currently in use is important for the development of new antimicrobials. The tetracyclines, discovered in the 1940s, are a well-established class of antibiotics that still have a role in treating microbial infections in humans. It is generally accepted that the main target of their action is the ribosome. The estimated affinity for tetracycline binding to the ribosomes is relatively low compared to the actual potency of the drug *in vivo*. Therefore, additional inhibitory effects of tetracycline on the translation machinery have been discussed. Structural evidence suggests that tetracycline inhibits the function of the essential bacterial GTPase Elongation Factor (EF)-Tu through interaction with the bound nucleotide. Based on this, tetracycline has been predicted to impede the nucleotide binding properties of EF-Tu. However, detailed kinetic studies of tetracycline's effect on nucleotide binding have been prevented by the fluorescence properties of the antibiotic. Here we report a fluorescence-based kinetic assay that minimizes the effect of tetracycline autofluorescence, enabling the detailed kinetic analysis of the nucleotide binding properties of *Escherichia coli* EF-Tu. Furthermore, using physiologically relevant conditions, we demonstrate that tetracycline does not affect EF-Tu's intrinsic or ribosome-stimulated GTPase activity, nor the stability of the EF-Tu•GTP•aa-tRNA complex. We therefore provide clear evidence that tetracycline does not directly impede the function of EF-Tu.

---

\* Published in PLOS ONE. The authors of the paper are Katherine E. Gzyl and Hans-Joachim. H-J.W. conceived the research; H-J.W. and K.E.G. designed the experiments; K.E.G. performed and analyzed the experiments; H-J.W. and K.E.G. wrote the paper.

## **Introduction**

Developing new antibiotics is a global priority due to antibiotic-resistant bacteria becoming more prevalent for common infections worldwide (56, 57). There has been great investment in developing new antibiotics from chemical libraries; however this route has not been overly successful (58, 59). The most promising route to developing new antibiotics to date has been through the modification of already known naturally produced antibiotics (58). However, resistance to these antibiotics usually occurs quickly because the respective resistance mechanisms are already present (59). An alternative approach would implement known antibiotic molecular mechanisms while screening chemical libraries and rationally designing new small molecule inhibitors (58, 60). However, from thousands of developed antibiotics, the molecular mechanism is only known for a few (29, 58). Furthermore, little is known about the secondary and non-specific targets of these antibiotics. One of these antibiotics is tetracycline.

Tetracycline is a broad spectrum antibiotic used in human and animal health with activity against a wide spectrum of pathogens (33, 61-63). While tetracycline use has declined due to increasing antibiotic resistance, many tetracycline derivatives have been developed based on the core molecular structure of tetracycline. Newly developed tetracycline derivatives can bypass current resistance mechanisms (33, 36, 64-66). All tetracyclines, except for atypical tetracyclines that target the bacterial cytoplasmic membrane, bind to the 30S ribosomal subunit and sterically block aminoacyl (aa)-tRNA from being accommodated into the A site (32, 33). The primary tetracycline binding pocket is formed by the irregular minor groove of helix 34 and the stem loop of helix 31 in the 16S rRNA (34-36). Tetracycline's polar edge interacts with the sugar phosphate

backbone of helix 34 and a magnesium ion, which coordinates indirect interactions with other nucleotides. A second magnesium ion coordinates interactions between tetracycline and helix 31. The hydrophobic face of tetracycline makes stacking interactions with bases of helix 34 (36). These unspecific interactions and the chelating properties of tetracycline are the reason why tetracycline binding can also be observed for a number of other secondary sites on the ribosome. The half maximal inhibitory concentration ( $IC_{50}$ ) in *in vitro* assays is  $\sim 10 \mu\text{M}$ ; however, minimal inhibitory concentration (MIC) of tetracycline to stop the growth of *E. coli* in culture  $\sim 1 \mu\text{M}$  (36, 41). This discrepancy between the MIC and  $IC_{50}$  in addition to the diverse resistance mechanisms for tetracycline, support the functional relevance of tetracycline binding to these secondary binding sites (36, 41).

Apart from targeting the bacterial ribosome, a tetracycline binding pocket has also been reported in EF-Tu, suggesting that tetracycline does indeed affect the function of EF-Tu directly (32, 42, 67-71). The recent structure of a 1:1 complex of trypsin-modified EF-Tu•GDP and tetracycline, solved using X-ray crystallography, supports a putative role of tetracycline in interfering with efficient nucleotide exchange *in vivo* (42). In the structure, tetracycline is bound to the GTPase domain and interacts with several key functional regions within conserved motifs found in the GTPase and ATPase super families (Figure 5). Briefly, tetracycline is coordinated through a magnesium ion, which is an essential co-factor for nucleotide binding in EF-Tu (72). The following features of EF-Tu are involved in hydrogen bonding interactions with tetracycline: the  $\alpha$ -phosphate of GDP, Thr25 (*Escherichia coli* numbering), and Asp80. Thr25 belongs to the conserved sequence of the phosphate binding (P)-loop ([G/A]X<sub>4</sub>GK[S/T]). Asp80 is part of the conserved switch II trigger sequence (DX<sub>2</sub>G). The Switch II trigger sequence and the P-

loop are the most important contributors to GTP binding in all GTPases and guanine nucleotide specificity is due to the Asp in the Switch II trigger sequence (73). Both these motifs are conserved in many ATPases and GTPases (74). In addition, a stacking interaction occurs between Pro82 and tetracycline. This proline residue is invariant in translational GTPases (75, 76). Based on the location and the amino acids that tetracycline interacts with in EF-Tu, it was predicted that nucleotide binding and GTP hydrolysis would be affected (42). Minor steric clashes in the superposition of the EF-Tu•GDP•tetracycline complex were observed and no steric clashes in the EF-Tu•EF-Ts complex (Figure 6 and 7) were observed (42). However, given that the P-loop and magnesium ion are important features in EF-Ts-stimulated nucleotide dissociation, the ability of EF-Ts to stimulate GDP dissociation might be impeded (Figure 7) (72, 77). For example, in EF-Tu nucleotide dissociation is initiated by the release of the phosphate end of the nucleotide (78). Further, since the tetracycline binding pocket is conserved in many GTPases and ATPases, additional essential proteins could be affected by tetracycline. It is estimated that 10-18% of all gene products are P-loop NTPases (79). In turn, this would explain the observed discrepancy between the MIC and IC<sub>50</sub> for *in vitro* translation assays.

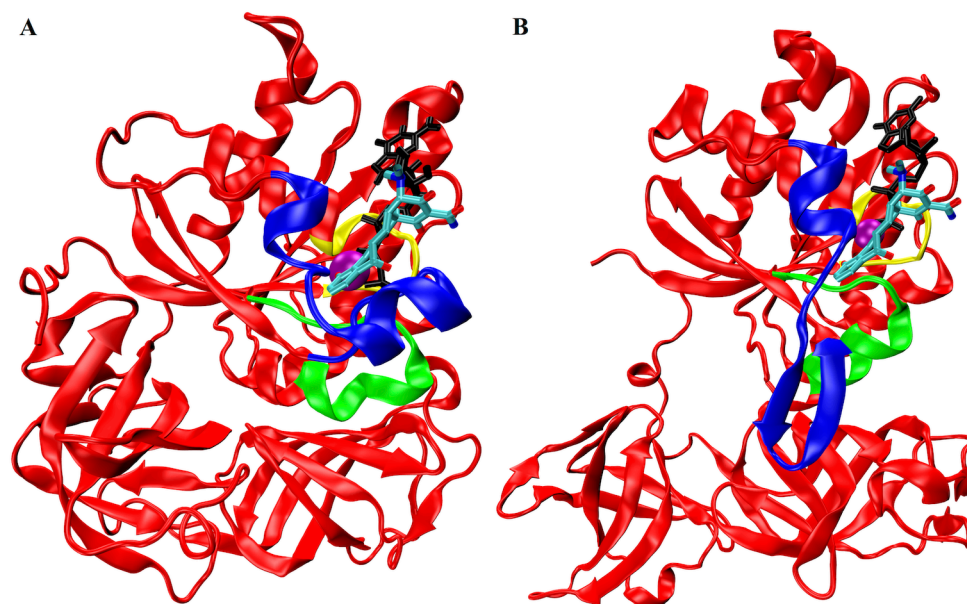


**Figure 6: Tetracycline binds proximal to switch I and II in EF-Tu.**

Cartoon illustration of the superposition of EF-Tu in the GTP state (panel A) and the GDP state (panel B) onto the trypsin-modified EF-Tu•GDP•tetracycline X-ray structure. Tetracycline is colored by atom, the magnesium ion is purple, switch I is highlighted in blue, switch II is highlighted in green, and the P-loop is highlighted in yellow. Panel (A) is the *E. coli* homology model of the crystal structure of *T. aquaticus* EF-Tu•GTP (PDB ID 1EFT) aligned to domain I of the EF-Tu•GDP•tetracycline crystal structure (PDB ID 2HCJ) (42). Panel (B) is the EF-Tu•GDP crystal structure (PDB ID 1EFC) (24) aligned to domain I of the EF-Tu•GDP•tetracycline crystal structure (PDB ID 2HCJ) (42).

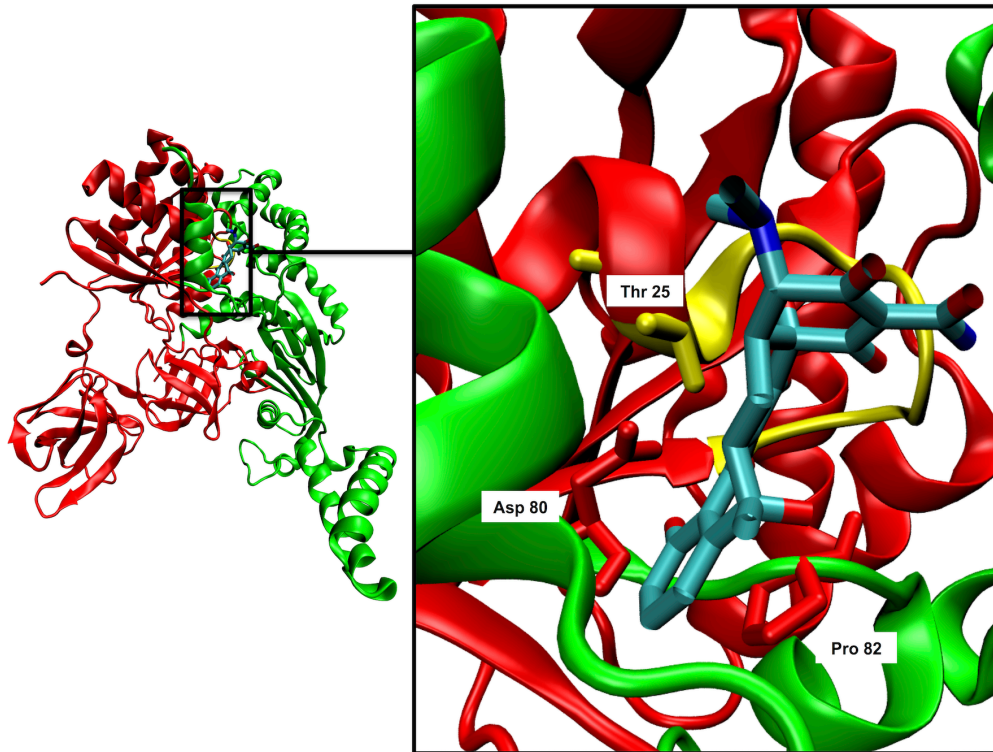


**Figure 7: Tetracycline binding is compatible with EF-Ts binding to EF-Tu.**

Interaction between tetracycline (colored by atom) bound EF-Tu (red) and EF-Ts (green) is represented using a cartoon illustration. The phosphate-binding loop is highlighted in yellow. Domain I of EF-Tu in the EF-Tu•EF-Ts (PDB ID 1EFU) (80) crystal structure was superimposed onto domain I of EF-Tu•GDP•tetracycline (PDB ID 2HCJ) (42).

Previously reported biochemical evidence suggests that tetracycline binding is able to modulate *E. coli* EF-Tu function (69, 70). Using fluorescence spectroscopy, the ability of tetracycline to bind both *E. coli* EF-Tu and *Sulfolobus solfataricus* EF-1 $\alpha$  was demonstrated (69). This study also provided evidence that tetracycline binding might have an effect on nucleotide affinity as well as the rate of GTP hydrolysis in EF-1 $\alpha$ . The effects of tetracycline on EF-1 $\alpha$  were slight (a  $\sim$ 1.5-fold reduction in nucleotide affinity at 50  $\mu$ M tetracycline and a  $\sim$ 25% decrease in the salt stimulated GTPase activity at 120  $\mu$ M tetracycline), but provided the basis for studying the effects of tetracycline on *E. coli* EF-Tu, which has a greater affinity for tetracycline than *S. solfataricus* EF-1 $\alpha$  (69). Due to the use of non-equilibrium methods, such as nitrocellulose filtration, and non-physiological conditions, such as salt stimulated GTPase activity, the results reported for *S. solfataricus* EF-1 $\alpha$  make it difficult to assess what effect tetracycline will have on the GTPase activity under *in vivo* conditions. Here, we adapted the fluorescence stopped-flow approach previously used (72, 77, 78, 81, 82) to study the kinetics of nucleotide binding in EF-Tu in order to gain detailed kinetic and thermodynamic information regarding the interaction of guanine nucleotides with EF-Tu in the presence of tetracycline. With the previously reported approach, it is not possible to observe the fluorescence of mant-labeled nucleotides in the presence of tetracycline due to the fluorescence properties of tetracycline (Figure 8). Furthermore, using purified components from the *E. coli* translation machinery, we were able to determine the intrinsic and ribosome stimulated GTPase activity of EF-Tu, as well as the stability of the ternary complex Phe-tRNA<sup>Phe</sup>•EF-Tu•GTP in the presence of tetracycline, avoiding the use of non-physiological, high salt conditions.



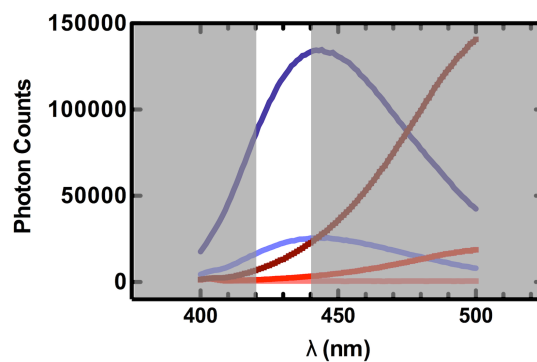


**Figure 8: Fluorescence emission properties of tetracycline and mant-nucleotides.**

Comparison of the emission spectra of tetracycline and mant-GTP with the transmittance range of the  $430 \pm 10$  nm bandpass filter (represented by the non-shaded areas). Three concentrations of tetracycline, 0.1  $\mu\text{M}$  (light pink), 10  $\mu\text{M}$  (red), and 100  $\mu\text{M}$  (dark red) and two concentrations of mant-GTP, 1  $\mu\text{M}$  (light blue) and 5  $\mu\text{M}$  (dark blue), were excited at a wavelength of 335 nm in Buffer C (*vide infra*).

To our knowledge, this is the first study that reports rate constants for the nucleotide binding kinetics of EF-Tu in the presence of tetracycline. The results reported here provide clear evidence that tetracycline does not affect translation through direct effects on the key enzymatic properties of EF-Tu, dismissing the observed interaction of tetracycline with EF-Tu as an exploitable target for antimicrobial drug development.

## **Materials and Methods**

### ***Expression and purification of EF-Tu and EF-Ts***

Proteins were expressed and purified to homogeneity as described in (81, 82). All purification steps contained GDP to prevent EF-Ts co-purification. The concentration of EF-Tu was determined with the extinction coefficient of  $32,900 \text{ M}^{-1}\text{cm}^{-1}$  at a wavelength of 280 nm. The EF-Tu extinction coefficient was determined with ProtParam (83). Protein purity was assessed by 12% SDS PAGE stained with Coomassie Brilliant Blue.

EF-Ts was expressed as a fusion protein from the IMPACT I system (NE Biolabs) provided by Charlotte Knudsen (Åarhus, Denmark) as described in (82) to homogeneity. The fusion protein contains a self-splicing intein and a chitin-binding domain that is removed during purification. The concentration and purity of EF-Ts were determined through 14% SDS stained with Coomassie Brilliant Blue and Image J was used to quantify the concentration through densitometry.

### ***Preparation of nucleotide free EF-Tu***

Nucleotide free EF-Tu was prepared as described in (81, 82). Briefly, EF-Tu•GDP was incubated with Buffer A (25 mM Tris-HCl, pH 7.5, 50 mM  $\text{NH}_4\text{Cl}$ , and 10 mM EDTA) at  $37^\circ\text{C}$  for 30 min to promote the dissociation of GDP. Then EF-Tu and GDP were separated on a Superdex 75 (GE healthcare) size exclusion column in Buffer B

(25 mM Tris-HCl, pH 7.5, and 50 mM NH<sub>4</sub>Cl). Fractions containing EF-Tu were collected and the concentration was quantified spectroscopically ( $\epsilon_{280}$  32,900 M<sup>-1</sup>cm<sup>-1</sup>). EF-Tu was diluted with Buffer C (50 mM Tris-HCl, pH 7.5, 70 mM NH<sub>4</sub>Cl, 30 mM KCl, and 7 mM MgCl<sub>2</sub>) prior to all experiments. All nucleotide-free EF-Tu was prepared the same day as rapid-kinetics assays were performed.

### ***Rapid-kinetics measurements***

A fluorescence stopped-flow apparatus (KinTek SF-2004) was used to determine rate constants as described in (72). Buffer C was used for all stopped-flow measurements. Nucleotide binding of EF-Tu was determined through fluorescence energy transfer from Trp184 ( $\lambda_{\text{ex}} = 280$  nm) in EF-Tu to the mant-group on either mant-GTP or mant-GDP. The fluorescence signal was detected after passing through a  $430 \pm 10$  nm bandpass filter (Edmund Optical).

Nucleotide association to EF-Tu is a second order reaction, which means that that the rate constant depends on both the concentration of mant-nucleotides and EF-Tu. However, pseudo first order conditions can be used so that the apparent first order rate constant depends on the concentration of only one of the reactants. Here, excess mant-GTP/mant-GDP was titrated against a constant concentration of nucleotide free EF-Tu ( $\sim 0.3$   $\mu\text{M}$ ). Under these pseudo first order conditions it was assumed that the concentration of mant-GTP/mant-GDP remained constant during the time course, and that the apparent first order rate constant was only dependent on the initial concentration of mant. The observable for the association reaction is then the formation of the EF-Tu•mant-GTP/GDP complex. Each apparent first order rate constant at a specific mant concentration was determined by fitting the following one-exponential function to

each fluorescence time course,

$$F = F_n + A \exp(-k_{app} \times t) \quad (1)$$

where  $F$  is fluorescence at time  $t$ ,  $F_n$  is the final fluorescence,  $A$  is amplitude and  $k_{app}$  is the apparent rate constant. The plot of the apparent rate as a function of the nucleotide concentration should be linear. A linear line indicates that under the conditions used the reaction is first order, and only depends on the initial concentration of mant-nucleotides. The slope of this line is the second order reaction rate constant. The association rate constant was determined by plotting the apparent rate as a function of the nucleotide concentration. For all association and dissociation experiments both syringes contained the appropriate concentration of tetracycline.

Dissociation rate constants were determined by forming an EF-Tu•mant-GTP/mant-GDP complex with 0.6  $\mu\text{M}$  EF-Tu and 6  $\mu\text{M}$  mant nucleotide (syringe concentrations). Then EF-Tu•mant-GTP/mant-GDP was chased with 60  $\mu\text{M}$  of unlabeled nucleotide. The dissociation rate constant was determined by fitting each time course to a one-exponential function (Equation 1). Nucleotide dissociation from EF-Tu is a first order reaction and the rebinding of unlabeled nucleotide is rapid, so the determined apparent rate was the rate constant.

The association reaction between EF-Tu•mant-GTP/GDP to EF-Ts also used pseudo first order conditions. For this reaction the concentration of EF-Ts was much greater than EF-Tu•mant-GTP/GDP. To observe the interaction between EF-Tu and EF-Ts, excess unlabeled nucleotides were added into the EF-Ts syringe allowing us to detect the interaction between the two proteins as a fluorescence decrease. Excess unlabeled nucleotide prevented the rebinding of mant. The pseudo first order rate constant of EF-Tu

EF-Tu•mant-GTP/GDP•EF-Ts complex formation was only dependent on the concentration of EF-Ts, which was assumed to remain constant through the experiment. The first portion of the  $k_{app}$  with respect to EF-Ts concentration was linear. This indicates that the formation of the EF-Tu•EF-Ts complex was rate limiting under these EF-Ts concentrations. If the concentration of EF-Ts had been further increased the plot would have reached saturation and plateaued (6). The  $k_{app}$  at saturation is the rate of EF-Tu•EF-Ts complex formation.

### ***GTPase assays***

The rate of GTP hydrolysis was determined as in (84). All GTPase assays were performed in Buffer C. Prior to measuring GTPase activity, [ $\gamma$ - $^{32}$ P]GTP (20  $\mu$ M) was charged for 15 min at 37 °C with phosphoenol pyruvate (3 mM), and pyruvate kinase (0.02  $\mu$ g/ $\mu$ L). Then EF-Tu (10  $\mu$ M) alone or together with EF-Ts (0.02  $\mu$ M or 0.2  $\mu$ M) was added and the reaction was incubated for 15 min at 37 °C. EF-Ts is added into the reaction mixture to prevent GDP dissociation from being the rate-limiting step. The reaction was allowed to cool to room temperature for 5 min. The reaction was started by the addition of the solution containing the appropriate concentration of tetracycline with no ribosomes, 70S ribosomes (0.1  $\mu$ M), or 50S ribosomal subunits (0.1  $\mu$ M). The 70S ribosome is composed of the 30S and 50S ribosomal subunits. EF-Tu binds the L12 stalk region and SRL on the 50S subunit (16, 17). At each time point, a 5  $\mu$ L aliquot of the reaction was quenched in 50  $\mu$ L of perchloric acid (1 M) and dipotassium phosphate (2 mM) to denature the proteins and RNA components so that they could no longer hydrolyze GTP. Free  $\gamma$ - $^{32}$ P was extracted using 400  $\mu$ L isopropyl and 300  $\mu$ L sodium molybdate (20 mM), because free  $\gamma$ - $^{32}$ P forms a complex with molybdate that is soluble in

the organic phase. The amount of hydrolyzed [ $\gamma$ - $^{32}\text{P}$ ]-GTP was determined by adding 200  $\mu\text{L}$  of the organic phase to 2 mL of scintillation cocktail (EcoLite, MP Biomedical) in 10 mL scintillation vials and scintillation counting (Tri-Carb 2800TR Perkin Elmer). Background radioactivity was determined and subtracted by using a reaction mixture that contained all components except EF-Tu.

### ***Hydrolysis protection assays***

The stability of the EF-Tu•GTP•aa-tRNA ternary complex was assessed as described in (81). The EF-Tu•GTP•aa-tRNA ternary complex was formed in Buffer D (50 mM Tris-HCl, pH 7.5 (4 °C), 70 mM  $\text{NH}_4\text{Cl}$ , and 10 mM  $\text{MgCl}_2$ ) with EF-Tu (1.5  $\mu\text{M}$ ), [ $^{14}\text{C}$ ]Phe-tRNA<sup>Phe</sup> (1.08  $\mu\text{M}$ ), GTP (1.5 mM), phosphoenol pyruvate (3 mM), and pyruvate kinase (0.17  $\mu\text{g}/\mu\text{L}$ ). [ $^{14}\text{C}$ ]Phe-tRNA<sup>Phe</sup> was prepared as described in (81) by incubating tRNA<sup>Phe</sup> (*E. coli* MRE 600, Sigma) with ATP (6 mM), inorganic pyrophosphatase (3 mM), phosphoenol pyruvate (3 mM), and pyruvate kinase (0.17  $\mu\text{g}/\mu\text{L}$ ) in Buffer E (25 mM Tris-Ac pH 7.5 (room temperature), 11 mM  $\text{Mg}(\text{OAc})_2$ , 100 mM  $\text{NH}_4\text{OAc}$ , 30 mM  $\text{MKOAc}$ , and 1 mM Dithiothreitol) for 30 min at 37 °C. Then [ $^{14}\text{C}$ ]-Phe (40  $\mu\text{M}$ ) and purified phenylalanyl-tRNA synthetase (~1  $\mu\text{M}$ ) was added to the solution, and incubated for 20 min at 37 °C. The reaction was quenched with the addition of 3 M KOAc (pH 4.5) to a final concentration of 0.3 M. Following the phenol/chloroform extraction, the RNA was precipitated with 2.5 volumes of cold (-20 °C) 100% ethanol overnight.

## Results and discussion

### The effect of tetracycline on the nucleotide binding properties of EF-Tu

The crystal structure of trypsin-modified EF-Tu•GDP•tetracycline revealed tetracycline bound to the GTPase (G)-domain of *E. coli* EF-Tu (Figure 5). Binding in this region was predicted to affect the ability of EF-Tu to bind and exchange guanine nucleotides (42). In an unrelated study, tetracycline was reported to decrease the affinity of guanine nucleotides (1.7- and 1.5-fold for GDP and GTP respectively) and this decrease in affinity was suggested to be the result of tetracycline affecting the association rate constant of GTP/GDP (69). Since tetracycline has a greater affinity for *E. coli* EF-Tu than *S. solfataricus* EF-1 $\alpha$ , we predicted the effect of tetracycline on nucleotide binding would be greater on *E. coli* EF-Tu. We therefore modified the previously reported stopped-flow approach, described in (72, 77, 78, 81, 82), to enable the direct analysis of guanine nucleotide association and dissociation kinetics in EF-Tu. The major challenge to this approach is the autofluorescence of tetracycline which, at sufficiently high concentrations, overwhelms the mant fluorescence signal that reports binding of the respective nucleotide to EF-Tu (72). A close inspection of the fluorescence spectra of mant-nucleotides and tetracycline when excited at 280nm reveals that the majority of the tetracycline autofluorescence occurs at wavelengths greater than 450nm, whereas the fluorescence maximum of mant lies at 440nm (Figure 8). In the past, mant fluorescence was recorded using 400nm long-pass cut-off filters. Based on these spectral properties, we used a  $430 \pm 10$  nm band-pass filter that is optimal to reduce tetracycline emission and still observe the fluorescence emission of the mant group (Figure 8) with high enough sensitivity to obtain time-resolved fluorescence changes of mant-GTP/GDP (Figure 9).

This modification of the well-established approach to dissect the nucleotide binding kinetics in *E. coli* EF-Tu (72, 77, 78, 81, 82), allowed us to study the association and dissociation of GTP and GDP, and EF-Ts-stimulated nucleotide exchange in EF-Tu according to the kinetic scheme shown in Figure 10.



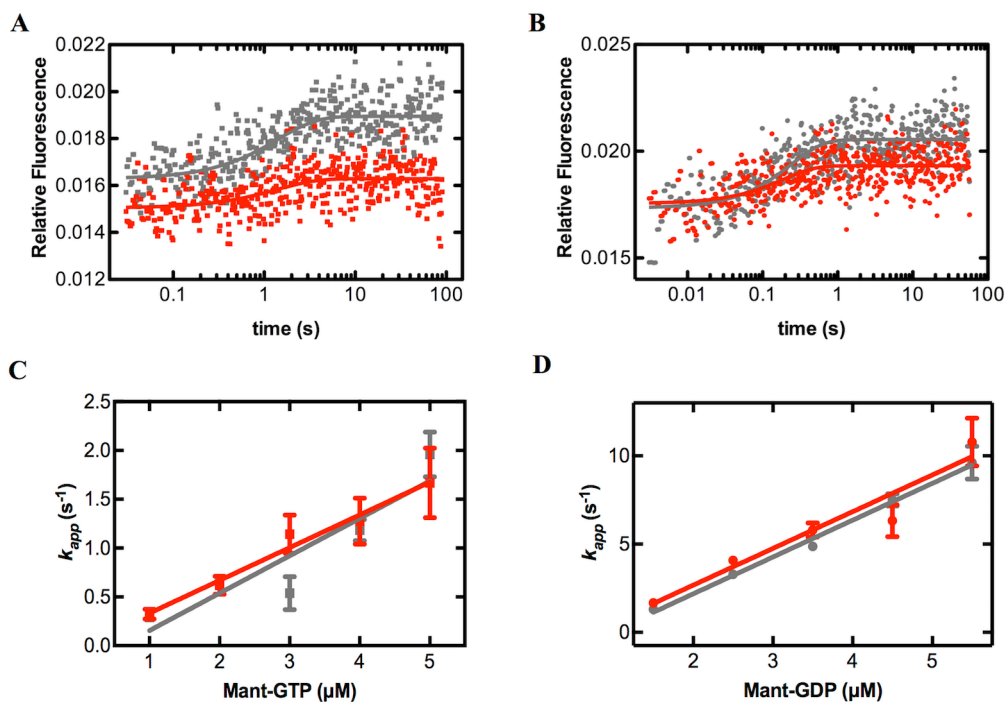


**Figure 9: Effect of tetracycline on the association rate of EF-Tu and mant-nucleotides.**

Representative time courses of (A) mant-GTP (2  $\mu\text{M}$ ) or (B) mant-GDP (2.5  $\mu\text{M}$ ) binding nucleotide free EF-Tu (0.3  $\mu\text{M}$ ) in the presence of either 0  $\mu\text{M}$  (grey) or 100  $\mu\text{M}$  (red) tetracycline measured by exciting the single tryptophan residue at 280 nm and observing fluorescent energy transfer to the mant group through a  $430 \pm 10$  nm band-pass filter. Concentration dependence of  $k_{\text{app}}$  for mant-GTP (C) or mant-GDP (D) in the presence of either 0  $\mu\text{M}$  tetracycline (grey) or 100  $\mu\text{M}$  tetracycline (red). Each  $k_{\text{app}}$  was determined by fitting time courses to a single exponential function, and the average of ( $n > 10$ ) time courses determined at a given nucleotide concentration is plotted. Error bars represent standard error.

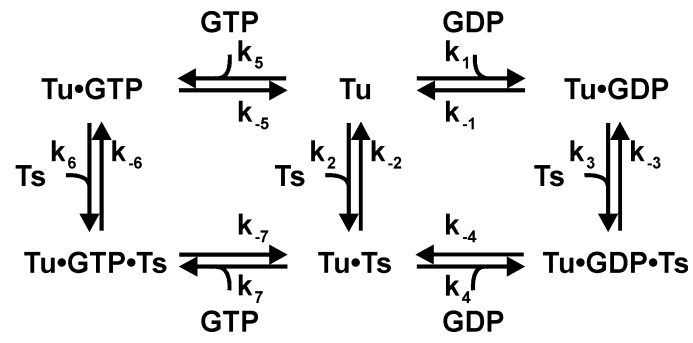


**Figure 10: Kinetic mechanism of nucleotide exchange in EF-Tu.**

### ***Nucleotide Association ( $k_1$ and $k_5$ )***

The association rate constants for GDP ( $k_1$ ) and GTP ( $k_5$ ) were determined by titrating mant-guanine nucleotides against a constant concentration of nucleotide free EF-Tu. At each nucleotide concentration, the apparent association rate constant was determined in the presence and absence of 100  $\mu$ M tetracycline (Figure 9C). By plotting the apparent rate constants with respect to nucleotide concentration, the association rate constant was determined (Table 1). The GTP association rate constant in the absence of tetracycline was  $k_5 = 3.9 \pm 0.1 \times 10^5 \text{ M}^{-1}\text{s}^{-1}$ , and the addition of 100  $\mu$ M tetracycline resulted in an unchanged rate constant ( $k_{5,\text{tet}} = 3.4 \pm 0.1 \times 10^5 \text{ M}^{-1}\text{s}^{-1}$ ). Both of these GTP association rate constants are in agreement with the previously reported rate constant of  $k_5 = 5 \pm 1 \times 10^5 \text{ M}^{-1}\text{s}^{-1}$  (72). Similarly, the GDP association rate constant of  $k_1 = 2.1 \pm 0.1 \times 10^6 \text{ M}^{-1}\text{s}^{-1}$  is not affected by the addition of 100  $\mu$ M tetracycline ( $k_{1,\text{tet}} = 2.1 \pm 0.3 \times 10^6 \text{ M}^{-1}\text{s}^{-1}$ ), and both rate constants agree with the earlier reported value of  $k_1 = 2.0 \pm 0.5 \times 10^6 \text{ M}^{-1}\text{s}^{-1}$  (72). Therefore, tetracycline has no effect on the association rate constants of either GTP or GDP to *E. coli* EF-Tu and, in turn, on the thermodynamics of this interaction.

**Table 1:** Kinetic parameters of nucleotide binding in EF-Tu in the presence of 0  $\mu\text{M}$  and 100  $\mu\text{M}$  tetracycline.

Condition	Rate
$k_1$	$2.1 \pm 0.1 \times 10^6 \text{ M}^{-1} \text{ s}^{-1}$
$k_{1, \text{tet}}$	$2.1 \pm 0.3 \times 10^6 \text{ M}^{-1} \text{ s}^{-1}$
$k_5$	$3.9 \pm 0.1 \times 10^5 \text{ M}^{-1} \text{ s}^{-1}$
$k_{5, \text{tet}}$	$3.4 \pm 0.1 \times 10^5 \text{ M}^{-1} \text{ s}^{-1}$
$k_{-1}$	$1.4 \pm 0.1 \times 10^{-3} \text{ s}^{-1}$
$k_{-1, \text{tet}}$	$1.2 \pm 0.1 \times 10^{-3} \text{ s}^{-1}$
$k_{-5}$	$1.4 \pm 1 \times 10^{-2} \text{ s}^{-1}$
$k_{-5, \text{tet}}$	$1.7 \pm 1 \times 10^{-2} \text{ s}^{-1}$
$k_3 / (1 + k_{-3} / k_{-4})$	$13.4 \pm 1.1 \times 10^6 \text{ M}^{-1} \text{ s}^{-1}$
$k_3 / (1 + k_{-3} / k_{-4})_{\text{tet}}$	$13.9 \pm 0.5 \times 10^6 \text{ M}^{-1} \text{ s}^{-1}$
$k_6 / (1 + k_{-6} / k_{-7})$	$21.9 \pm 1.4 \times 10^6 \text{ M}^{-1} \text{ s}^{-1}$
$k_6 / (1 + k_{-6} / k_{-7})_{\text{tet}}$	$19.8 \pm 1.1 \times 10^6 \text{ M}^{-1} \text{ s}^{-1}$

#### ***Nucleotide dissociation ( $k_{-1}$ and $k_{-5}$ )***

The dissociation rate constants for GDP ( $k_{-1}$ ) and GTP ( $k_{-5}$ ) were measured by chasing EF-Tu•mant-GTP/mant-GDP with excess unlabeled GTP/GDP (72). Under these conditions, dissociation of the mant-labeled nucleotide is rate limiting and the binding of unlabeled nucleotide is rapid, effectively preventing rebinding of the labeled nucleotide. Therefore, the observed dissociation rate is the rate constant of this first-order dissociation reaction ( $k_{-1}$ ,  $k_{-5}$ ). Figure 11A shows the obtained dissociation time course of GDP in the absence of tetracycline. When carried out in the presence of increasing concentrations of tetracycline, no change of the rate constant for either GTP ( $k_{-5} = 0.017 \pm 0.003 \text{ s}^{-1}$ ) or GDP ( $k_{-1} = 0.0012 \pm 0.0001 \text{ s}^{-1}$ ) was observed (Figure 11B). The obtained dissociation rate constants (summarized in Table 1) agree with the previously reported rate constants of  $k_{-5} = 0.03 \pm 0.01 \text{ s}^{-1}$  for GTP and  $k_{-1} = 0.002 \pm 0.001 \text{ s}^{-1}$  for GDP dissociation. These results demonstrate that tetracycline

does not interfere with the spontaneous release of guanine nucleotides from EF-Tu ( $k_{-1}$  and  $k_{-5}$ ).

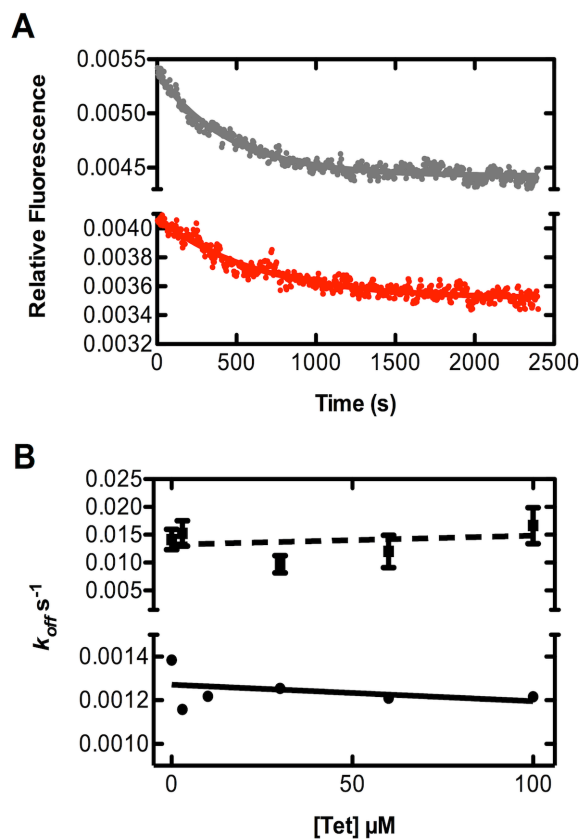


**Figure 11: Effect of tetracycline on the dissociation rate of EF-Tu and mant-nucleotides.**

Panel (A) shows a representative time course of GTP dissociation from EF-Tu (0.3 μM) in the presence of either 0 μM tetracycline (grey trace) or 100 μM tetracycline (red trace). The concentration dependence of the  $k_{-5}$  (GTP, ■ symbols and broken line) or  $k_{-1}$  (GDP, ● symbols and solid line) as a function of tetracycline concentration is shown in panel (B). Fluorescence energy transfer was monitored by exciting the single tryptophan residue present in EF-Tu and monitoring mant fluorescence through a  $430 \pm 10$  nm bandpass filter. Each rate constant is an average of ( $n > 9$ ) time courses fit to a single exponential function, and error bars are standard errors.

***EF-Ts stimulated nucleotide dissociation from EF-Tu ( $k_3 / (1 + k_{-3} / k_{-4})$  and  $k_6 / (1 + k_{-6} / k_{-7})$ )***

Under *in vivo* conditions, the exchange of nucleotides in EF-Tu requires an additional translation factor, EF-Ts. The action of nucleotide exchange factor EF-Ts is required due to the fact that spontaneous dissociation of nucleotides, in particular GDP, from EF-Tu is too slow to sustain *in vivo* protein synthesis rates. To investigate a potential effect of tetracycline on this physiologically relevant step, we performed an EF-Ts titration of the stimulated nucleotide exchange reaction. We determined the apparent rate of nucleotide dissociation from EF-Tu at increasing concentrations of EF-Ts in the presence of a constant amount of EF-Tu•mant-GTP/mant-GDP, similar to the approach describe above (72). Consistent with the coupled equilibria in Figure 10, we observed a linear initial phase (Figure 12) under low concentrations of EF-Ts, which represents the combined rate constants for the formation of the EF-Tu•GTP/GDP•EF-Ts complex and the dissociation of the nucleotide (Figure 10). This approach allows us to assay if any of the EF-Ts related steps are affected by tetracycline, as a change in the rate constant of either of the contributing steps will alter the slope of the concentration dependence. Interestingly, the slope of the combined rate constants in the presence and absence of 100  $\mu$ M tetracycline is unchanged (summarized in Table 1). The value of the combined rate constants for stimulated GTP dissociation was  $k_6 / (1 + k_{-6} / k_{-7}) = 21.9 \pm 1.4 \times 10^6 \text{ M}^{-1}\text{s}^{-1}$  in the absence of tetracycline and  $k_6 / (1 + k_{-6} / k_{-7})_{\text{tet}} = 19.8 \pm 1.1 \times 10^6 \text{ M}^{-1}\text{s}^{-1}$  in the presence of 100  $\mu$ M tetracycline. Both of these values agree with earlier reported work ( $k_6 / (1 + k_{-6} / k_{-7}) = 20 \times 10^6 \text{ M}^{-1}\text{s}^{-1}$ ) and indicate that tetracycline does not affect EF-Ts stimulated dissociation of GTP from EF-

Tu (72). Similarly, the combined rate constants for the stimulated dissociation of GDP were determined to be  $k_3 / (1 + k_{-3} / k_{-4}) = 13.4 \pm 1.1 \times 10^6 \text{ M}^{-1}\text{s}^{-1}$  in the absence of tetracycline and  $k_3 / (1 + k_{-3} / k_{-4})_{\text{tet}} = 13.9 \pm 0.5 \times 10^6 \text{ M}^{-1}\text{s}^{-1}$  in the presence of 100  $\mu\text{M}$  tetracycline, which is in excellent agreement with the reported value of  $k_3 / (1 + k_{-3} / k_{-4}) = 16 \times 10^6 \text{ M}^{-1}\text{s}^{-1}$  (72). Therefore, our results indicate that tetracycline does not affect either the interaction of EF-Tu and EF-Ts ( $k_{-3}$  and  $k_{-6}$ ) or the subsequent nucleotide release steps from the EF-Tu•GTP/GDP•EF-Ts ternary complex ( $k_4$ ,  $k_{-4}$  and  $k_7$ ,  $k_{-7}$ ).



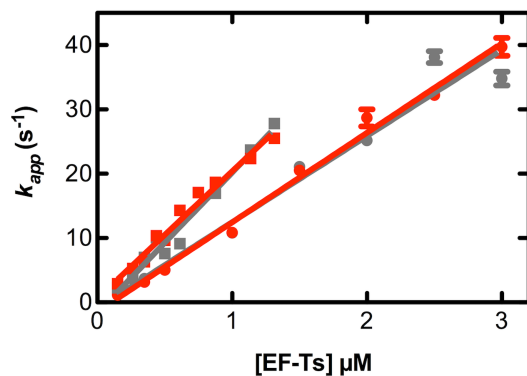


**Figure 12: Effect of tetracycline on EF-Ts-stimulated dissociation of mant-nucleotides from EF-Tu.**

The EF-Ts dependence of the dissociation rates for mant-GTP (■) and mant-GDP (●) from EF-Tu (0.15 μM) is shown in the presences (red) and absence (gray) of 100 μM tetracycline. Fluorescence energy transfer from the mant group to the single tryptophan in EF-Tu was observed through a  $430 \pm 10$  nm band-pass filter by exciting the single tryptophan in EF-Tu at 280 nm. Each  $k_{app}$  is the average ( $n > 11$ ) of time courses at that EF-Ts concentration. The error bars indicate the standard error.

In summary, the detailed kinetic analysis of the nucleotide binding properties of EF-Tu in the presence of up to 100  $\mu\text{M}$  tetracycline support the notion that this essential step in the functional cycle of EF-Tu is not affected by tetracycline. The tetracycline concentration used here is much greater than the peak plasma concentration of a single standard administered dose of tetracycline in humans, which is 1.02  $\mu\text{g/mL}$  (2.29  $\mu\text{M}$ ) (85). Therefore, we feel confident that tetracycline does not target nucleotide binding in EF-Tu as part of its mode of action. Our results are in contrast to data reported by Lamberti et al (2011), which reported a slight (1.7- to 1.5-fold) decreased affinity in EF-1 $\alpha$  for guanine nucleotides in the presence of 50  $\mu\text{M}$  tetracycline. However, non-equilibrium methods were used by Lamberti et al and the effect on the association rate constant was not directly measured (69). Furthermore, our observations are supported by a computational study suggesting that tetracycline binding to EF-Tu causes only a small change in free energy and is facilitated indirectly via the magnesium ion and GDP (67).

#### **Tetracycline has no effect on the GTPase activity of EF-Tu**

Although the nucleotide binding properties of EF-Tu are not altered in the presence of tetracycline, the fact that tetracycline binds to the G domain of EF-Tu and interacts with the P-loop and the switch II trigger sequence (Figure 6) gave rise to the hypothesis that its mode of action might include a direct effect on GTP hydrolysis by EF-Tu (42, 86). Consistent with such a role, the previously reported salt-stimulated GTPase activity of *S. solfataricus* EF-1 $\alpha$  was reduced by  $\sim 25\%$  in the presence of 120  $\mu\text{M}$  tetracycline (69). However, decreasing the already extremely slow intrinsic GTP-hydrolysis rate of EF-Tu seems like an unlikely additional mode of tetracycline antibiotic action. To investigate this further, we used physiologically relevant buffer conditions to

determine if tetracycline had an effect, not only on the intrinsic, but also on the 70S ribosome and 50S ribosomal subunit-stimulated GTPase activity of EF-Tu.

### ***Intrinsic GTPase activity***

To learn if tetracycline is able to modulate the intrinsic GTP hydrolysis reaction of EF-Tu, we determined the multiple turnover GTPase activity of EF-Tu at increasing concentrations (up to 500  $\mu\text{M}$ ) of tetracycline. Rates of multiple turnover GTP hydrolysis ( $k_{\text{GTPase}}$ ) were determined from the initial linear phase of the time course, both in the presence and absence of tetracycline (Figure 13A, Table 2). Our results in the absence of tetracycline are consistent with previous work using the same buffer (84). In addition, increasing the tetracycline concentration up to 500  $\mu\text{M}$  (Figure 13B) did not reduce the observed multiple turnover hydrolysis rate of intrinsic GTP hydrolysis (summarized in Table 2). This further supports our observation that tetracycline at concentrations higher than 100  $\mu\text{M}$  is not interfering with the EF-Ts-mediated nucleotide exchange reaction. Furthermore, our results presented here demonstrate that tetracycline, although binding in the vicinity of the  $\gamma$ -Phosphate of the bound GTP, does not alter the intrinsic GTPase activity of EF-Tu.

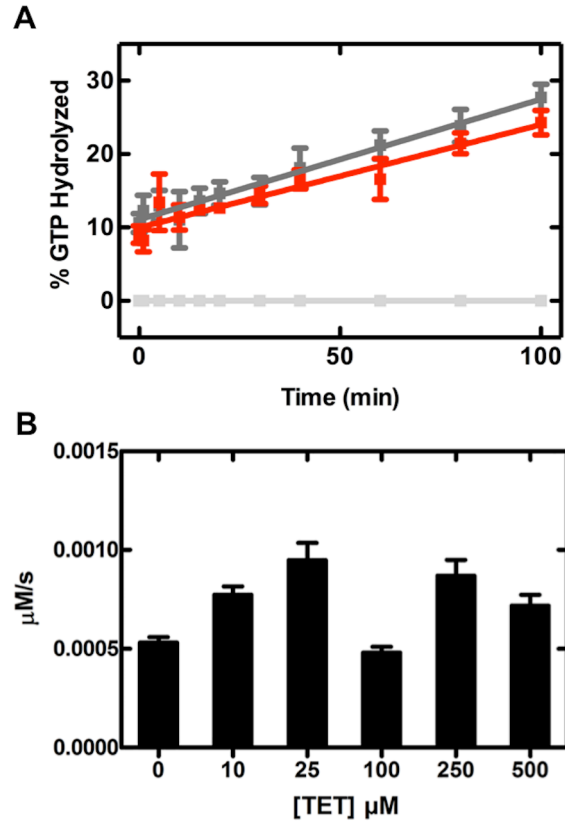


**Figure 13: Effect of tetracycline on the intrinsic GTPase activity.**

The linear phase of time courses of reactions using 10  $\mu\text{M}$  EF-Tu and 0.2  $\mu\text{M}$  EF-Ts are plotted in panel (A) for 0  $\mu\text{M}$  (grey) and 100  $\mu\text{M}$  (red) tetracycline. The rate of hydrolysis at different tetracycline concentrations is shown in Panel (B). Data plotted is an average ( $n = 3$ ) and the error bars indicate the standard error.

**Table 2:** Effect of 100  $\mu\text{M}$  tetracycline on the intrinsic, 70S-, and 50S-stimulated GTPase activity of EF-Tu.

Condition	Rate ( $\mu\text{M s}^{-1}$ )
$k_{\text{GTPase}}$	$7.67 \pm 1.33 \times 10^{-4}$
$k_{\text{GTPase, tet}}$	$6.67 \pm 1.33 \times 10^{-4}$
$k_{\text{GTPase, 0.02 } \mu\text{M EF-Ts}}$	$5.33 \pm 0.67 \times 10^{-4}$
$k_{\text{GTPase, 0.02 } \mu\text{M EF-Ts, tet}}$	$4.67 \pm 0.67 \times 10^{-4}$
$k_{\text{GTPase, 0.2 } \mu\text{M EF-Ts}}$	$5.33 \pm 0.33 \times 10^{-4}$
$k_{\text{GTPase, 0.2 } \mu\text{M EF-Ts, tet}}$	$4.67 \pm 0.33 \times 10^{-4}$
$k_{\text{GTPase, 70S}}$	$2.67 \pm 0.20 \times 10^{-3}$
$k_{\text{GTPase, 70S, tet}}$	$2.17 \pm 0.23 \times 10^{-3}$
$k_{\text{GTPase, 50S}}$	$1.0 \pm 0.3 \times 10^{-3}$
$k_{\text{GTPase, 50S tet}}$	$1.3 \pm 0.3 \times 10^{-3}$

### ***Ribosome-stimulated GTPase activity***

The multiple turnover GTPase activity of EF-Tu can be stimulated  $\sim 2$ -fold by the presence of empty 70S ribosomes (70, 84), providing a sensitive measure for tetracycline interfering with the interaction of EF-Tu•GTP. Similar to the reported intrinsic GTPase activity, rates of hydrolysis were determined from the initial phase of the respective GTP hydrolysis time courses. The 70S-stimulated multiple turnover GTP hydrolysis activity of EF-Tu was  $k_{\text{GTPase, 70S}} = 2.67 \pm 0.20 \times 10^{-3} \mu\text{M s}^{-1}$  (Figure 14A and Table 2). In the presence of increasing concentrations of tetracycline, up to 500  $\mu\text{M}$  (Figure 14B), the multiple turnover GTP hydrolysis activity remains essentially unaffected. With a  $k_{70\text{S, tet}}$  at 100  $\mu\text{M}$  of  $2.17 \pm 0.23 \times 10^{-3} \mu\text{M s}^{-1}$  the rate of 70S-stimulated GTPase activity in EF-Tu is similar under all tetracycline conditions tested. Consistent with this, the 50S-stimulated GTP-hydrolysis activity of EF-Tu is unaffected by 100  $\mu\text{M}$  tetracycline ( $k_{50\text{S}} = 1.0 \pm 0.3 \times 10^{-3} \mu\text{M s}^{-1}$  and  $k_{50\text{S, tet}} = 1.3 \pm 0.3 \times 10^{-3} \mu\text{M s}^{-1}$ ), summarized in Figure 14C and Table 2). This is not surprising, as the 70S-stimulated GTPase activity of EF-Tu is mainly due to the interaction of EF-Tu with GTPase Activating Center (GAC and the

sarcin-ricin loop (SRL), including ribosomal proteins L7/L12 located on the 50S (87). Our finding that the 70S ribosome, which is the cellular target of EF-Tu, is able to stimulate the GTPase activity of EF-Tu even at 500  $\mu$ M is in contrast to Lamberti et al (2011) who reported an effect of tetracycline on the ribosome-independent salt-stimulated GTPase activity of EF-1 $\alpha$ . The observed 25% reduction might be specific to their use of 3.6 M NaCl to stimulate the GTPase activity of *S. solfataricus* EF-1 $\alpha$ . The physiologically irrelevant salt-stimulated GTPase activity could involve a different mechanism, which might be sensitive to the presence of tetracycline.

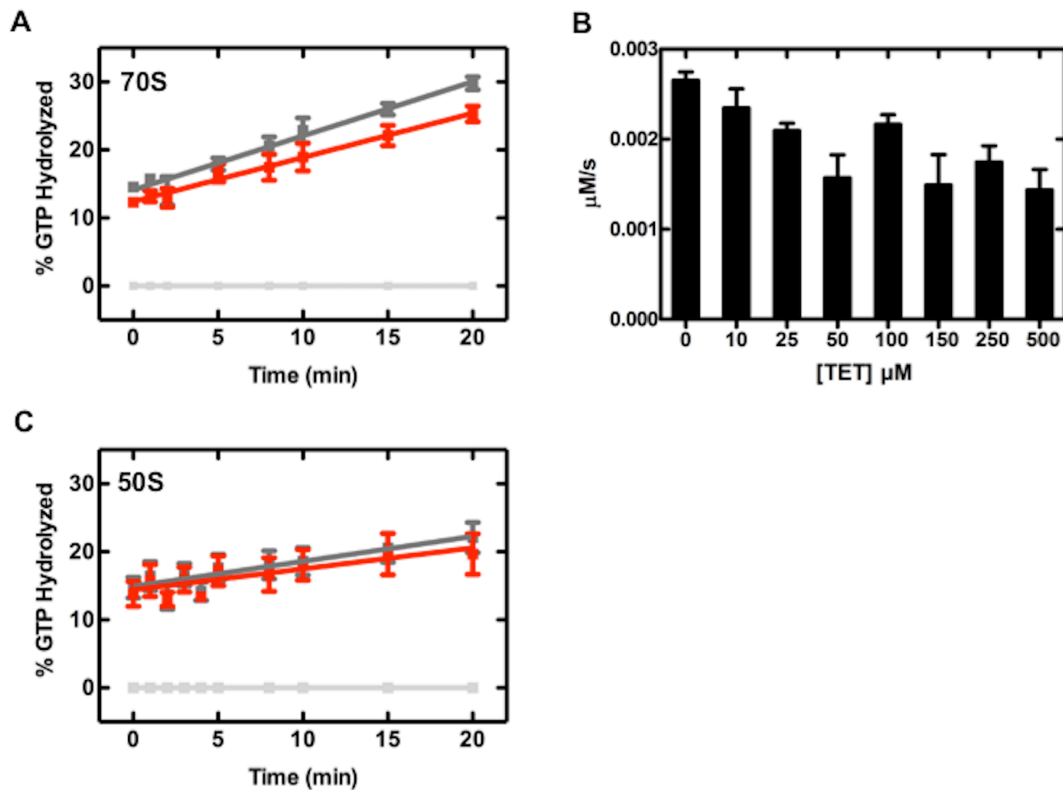


**Figure 14: Ribosome-stimulated GTPase activity.**

Effect of tetracycline on the 70S (0.1 μM) and 50S (0.1 μM) -stimulated GTPase activity of EF-Tu (10 μM) with EF-Ts (0.02 μM). Panel (A) is the linear phase of the time course for GTP hydrolysis of EF-Tu stimulated by the 70S ribosome in the presence (100 μM) and absence of tetracycline. Panel (B) shows the dependence of the rate of GTP hydrolysis on the concentration of tetracycline. The linear phase of 50S stimulated GTP hydrolysis reaction is plotted in panel (C) in the presence (100 μM) and absence of tetracycline. Each point on the plots is the average of (n=3) independent experiments and the error bars represent the standard error.

### **Tetracycline does not alter EF-Tu•GTP•aa-tRNA stability**

In the active GTP bound state, EF-Tu has a high affinity for aa-tRNA ( $K_D \approx 10^{-8}$  M) and forms the EF-Tu•GTP•aa-tRNA ternary complex (88). The interaction between aa-tRNA and EF-Tu involves binding of the aminoacylated 3' end of the tRNA into the cleft between domains I and II. The 5' end of the tRNA body is bound by the junctions of the three domains of EF-Tu (89). While the aa-tRNA is bound by EF-Tu as part of the ternary complex (Figure 15A), the aminoacyl-ester bond between the amino acid and the tRNA body is protected from spontaneous hydrolysis (~10-fold) by the interaction with EF-Tu (81). This effect is highly sensitive to structural perturbation of the amino acid binding pocket as well as slight changes in the on and off rates of the aa-tRNA. Since the tetracycline binding site is proximate to switch I and II which undergo structural rearrangements upon GTP binding to EF-Tu and form part of the aa-tRNA interaction surface of EF-Tu, we wanted to investigate if binding of tetracycline to EF-Tu might perturb the aa-tRNA interaction. To this end, we monitored the stability of the aminoacyl-ester bond as previously described (35) in the presence of increasing tetracycline concentrations (Figure 15). As reported by De Laurentiis et al (2011), the half-life of the [ $^{14}$ C]Phe-tRNA<sup>Phe</sup> was ten-fold greater in the presence of EF-Tu•GTP than in the absence of EF-Tu (15). Increasing the tetracycline concentration to 100 $\mu$ M had no effect on EF-Tu's ability to protect the highly sensitive aminoacyl-ester bond against spontaneous hydrolysis (Figure 15B and Table 3). This is supported by the observation that tetracycline does not impede the delivery of the EF-Tu•GTP•aa-tRNA ternary complex to ribosomes (32). This observation suggests that either tetracycline binds to *E. coli* EF-Tu



and does not affect aa-tRNA binding or that tetracycline does not have a high enough affinity to the ternary complex under physiologically relevant conditions.

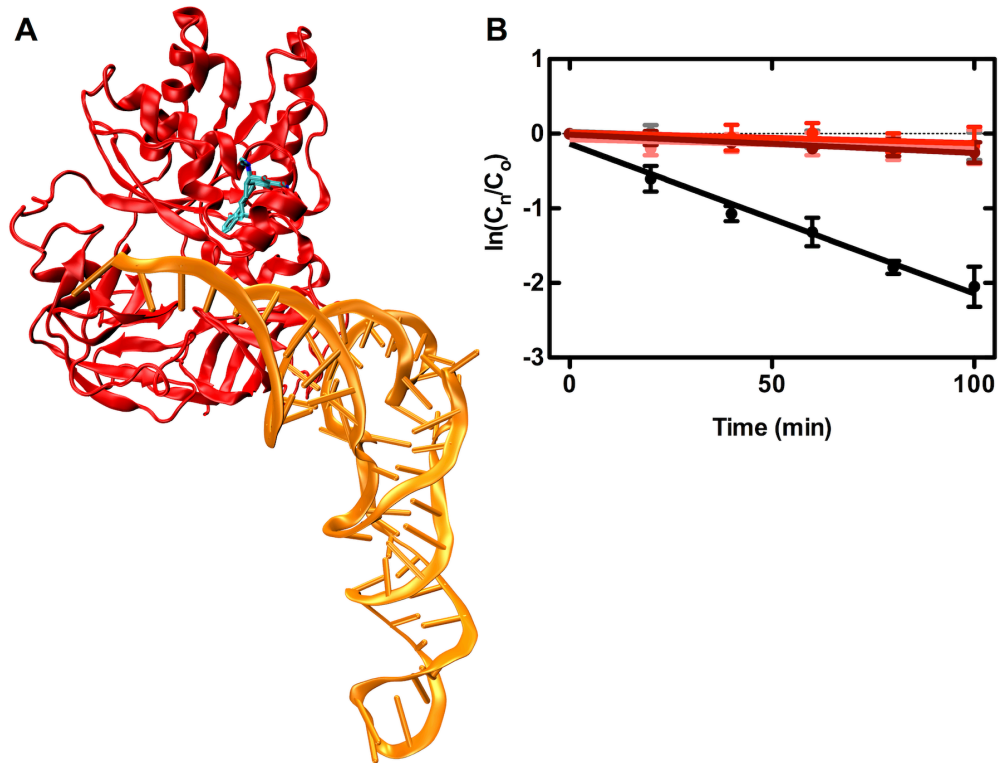


**Figure 15: Effect of tetracycline on aminoacyl-tRNA protection by EF-Tu.**

(A) Model of the EF-Tu•GTP•aa-tRNA complex interacting with tetracycline. EF-Tu is shown in red and Phe-tRNA<sup>Phe</sup> is orange, and tetracycline is colored by atom. The crystal structure of the EF-Tu•GTP•aa-tRNA complex (PDB ID 1OB2) was superimposed onto domain I of the EF-Tu•GDP•tetracycline complex (PDB ID 2HCJ). (B) Time dependence of the spontaneous hydrolysis of the amino-ester bond obtained by incubating Phe-tRNA<sup>Phe</sup> (1.08  $\mu$ M) at 37°C with no EF-Tu (black), with EF-Tu•GTP (1.5  $\mu$ M) and no tetracycline (grey), with EF-Tu•GTP (1.5  $\mu$ M) and 30  $\mu$ M tetracycline (red), or EF-Tu•GTP (1.5  $\mu$ M) and 100  $\mu$ M tetracycline (brown).

**Table 3:** Effect of tetracycline on the ability of EF-Tu to protect the amino-ester bond in Phe-tRNA<sup>Phe</sup>.

Condition	Half life (min)
No EF-Tu	35 ± 4
EF-Tu 0μM Tet	382 ± 64
EF-Tu 3μM Tet	542 ± 46
EF-Tu 30μM Tet	483 ± 45
EF-Tu 100μM Tet	282 ± 72

### Conclusion

Our data reported here demonstrates that tetracycline does not affect the nucleotide binding properties of EF-Tu, nor the ability of EF-Ts to stimulate nucleotide dissociation. Furthermore, no effect on the intrinsic, 70S- and 50S-stimulated multiple turnover GTP hydrolysis activity of EF-Tu could be detected. Similarly, the formation or stability of the EF-Tu•GTP•aa-tRNA ternary complex is insensitive to the presence of tetracycline in physiologically relevant conditions. Based on the reported data, we feel confident stating that during therapeutic use of tetracycline, EF-Tu is not a direct target of the antibiotic because the concentrations used in our work are much higher than the peak plasma concentration of tetracycline (85). Our observations suggest that although tetracycline is able to bind to the trypsin-modified fragment of EF-Tu, which does not contain a switch I loop, tetracycline either does not have an influence on the functional cycle of EF-Tu or that, for example when the switch 1 loop is present, it cannot bind to EF-Tu. As a consequence, direct tetracycline binding to EF-Tu as an exploitable target for antimicrobial drugs should likely be dismissed.

The reported binding pocket of tetracycline is conserved in many other GTPases and ATPases. However, the predicted main contributor of tetracycline binding to EF-Tu is the conserved, nucleotide-bound magnesium ion, and no amino acids make a

significant contribution to the free energy of binding (67). If tetracycline binds other GTPases and ATPases through a divalent metal ion interaction in a similar binding pocket as in EF-Tu, it is unlikely that tetracycline will exert a functional effect. Therefore, the observed discrepancy between the MIC and  $IC_{50}$  for tetracycline is unlikely to be caused by tetracycline binding to other GTPases or ATPases either. Thus, the other tetracycline binding sites on the 30S and 50S ribosomal subunits might be responsible for the observed effectiveness of tetracycline as drug, likely through perturbation of different processes such as ribosome biogenesis or translation termination (35, 40).

### **Chapter 3: Macromolecular crowding affects the nucleotide binding properties of elongation factor-Tu\***

#### **Abstract**

Cells are inherently crowded, and the function of macromolecules in a cell evolved in this crowded matrix. In bacteria, EF-Tu controls the speed and accuracy of translation. The function of EF-Tu is well studied in dilute conditions, but nothing is known about how the crowded environment of the cell influences EF-Tu's function. Here, we investigate the effect of macromolecular crowding on EF-Tu using the synthetic inert polymers dextran 40 and PEG 4000. This approach allows us to focus on the effect of volume exclusion, because these crowders have been reported to reduce the contribution of nonspecific interactions. Using rapid-kinetics and the stopped-flow technique, we have determined the nucleotide-binding properties of EF-Tu in the presence of increasing concentrations of these crowding agents. This detailed kinetic analysis of the nucleotide association and dissociation rate constants reveals that macromolecular crowding induced by both Dextran 40 and PEG 4000 decreases the affinity of EF-Tu for GTP and increases the affinity of EF-Tu for GDP. However, the osmolyte glucose decreases both association and dissociation rates for GTP and GDP similarly. Since volume exclusion compacts flexible regions, we performed molecular dynamics simulations of both nucleotide bound forms of EF-Tu to determine which state would be more affected by crowding. A role of

---

\* This manuscript has not been submitted. The authors of the manuscript are Katherine E. Gzyl, Dylan Girodat and Hans-Joachim Wieden. K.E.G. and H-J.W. conceived the research; H-J.W. and K.E.G. designed the experiments; K.E.G. performed and analyzed the stopped-flow experiments; D.G. performed the molecular dynamics simulations and calculated the RMSF; K.E.G used the RMSF values to color EF-Tu by flexibility, and to predict flexible regions in EF-Tu; K.E.G. and H-J.W wrote the manuscript.

crowding in regulation protein synthesis rates is discussed.

## **Introduction**

The bacterial GTPase elongation factor (EF)-Tu has evolved its functional properties in the crowded environment of the cell (8). For instance, it was estimated that the cytoplasm of *Escherichia coli* contains a concentration between 300g/L to 400g/L (20-30% volume occupancy) of protein and RNA depending on the growth phase (47). Further, it was estimated that *E. coli* K12 contains 200g/L of protein, 75g/L of RNA and 10-20g/L of DNA (90). Consistent with this is the observation that in order to replicate processes such as DNA replication (91), transcription and translation (92), and ribosome reconstitution from coupled transcription-translation systems (49) *in vitro*, crowded environments are needed. These crowded conditions can be achieved by the use of synthetic polymers (dextran, (poly)ethylene glycol (PEG), Ficoll) or natural proteins (bovine serum albumin, lysozyme, ovalbumin) depending on the macromolecule under investigation. Yet, *in vitro* most proteins including EF-Tu are studied at concentrations below 1g/L (6, 44-46). Although considerable evidence exists suggesting effects of crowding on biomolecular function, it is unknown how macromolecular crowding affects the function of any translational GTPase including EF-Tu.

EF-Tu is an essential translational GTPase, that is stimulated by the ribosome (9). EF-Tu consists of three domains (G domain or domain I, domain II, and domain III) that reorient depending on the nucleotide bound state (Figure 5). The conformational change from the GTP-bound active state to the GDP-bound inactive state involves substantial structural reorientations of the three domains where EF-Tu transitions from a compact

closed state to an open state (11, 93). GTP-bound EF-Tu has a high affinity for aminoacyl (aa)-transfer (t)RNA and forms the EF-Tu•GTP•aa-tRNA ternary complex (94). In this complex, EF-Tu delivers aa-tRNA to the translating 70S ribosome in a codon-dependent fashion (32). After correct codon-anticodon recognition EF-Tu rapidly hydrolyzes GTP, relaxes from the tight GTP conformation to the more open GDP conformation followed by P<sub>i</sub>-release, and then releases the bound aa-tRNA into the ribosomal A site (23). When in the GDP conformation, the affinity for aa-tRNA is significantly decreased (94). In order to exchange the bound GDP for GTP, enabling EF-Tu to participate in another round of translation, it binds to its guanine exchange factor (GEF) EF-Ts, which accelerates dissociation of GDP over 6000-fold (6). Subsequent GTP binding is driven by the high cellular concentration of the nucleotide and the formation of the EF-Tu•GTP•aa-tRNA complex (95). Interestingly, EF-Tu has approximately 100-fold higher affinity for GDP than for GTP (6). We hypothesize that the difference in conformation of the GTP and GDP states should render EF-Tu's functional cycle sensitive to the concentration of biomolecules in the cytosol acting as crowding agents. These cellular crowders should affect the GTP- and GDP-bound conformations of EF-Tu differently due to the well-studied effect of crowding agents compacting flexible regions more than rigid regions in proteins (5, 54, 55).

Macromolecular crowding leads to volume exclusion, confinement, and nonspecific interactions between the crowders and the macromolecule of interest (52, 96). Macromolecules exclude volume from each other by the principle that the space occupied by one molecule cannot be simultaneously occupied by another molecule. Excluded volume lowers the entropy of non-compact states more than compact states, thus compact

states will be more stabilized than non-compact states (52). Under crowded conditions, as observed in *E. coli*, volume exclusion is the dominant effect (96, 97). For example, different sizes and concentrations PEG were used to determine the effect of macromolecular crowding on the ATPase activity and structure of the translational helicase eukaryotic initiation factor (eIF)4A. The overall shape of eIF4A is compacted and is more similar to the close active conformation under crowded conditions. This resulted in an increased rate of ATP hydrolysis (55). Another study revealed that phosphoglycerate kinase is compacted by Ficoll 70 in a manner that brings together its N and C-termini together to increase the reaction rate (5). The reaction rate is increased because the N-termini, which contains the ADP binding site, and the C-termini, which contains the diphosphoglycerate binding site, must come together for ATP product formation (5). The role of nonspecific interactions such as electrostatic, hydrophobic and van der Waals, occurring between crowding agents and the probe molecule is difficult to interpret because they depend on the specific chemical groups on the crowding agent as well as the macromolecule under study (52, 97, 98). Synthetic inert polymers are often used to mimic the effect of macromolecular crowding while eliminating some of the nonspecific interactions (51, 99). For this reason we selected dextran 40 and PEG 4000 to study the guanine nucleotide-binding properties of EF-Tu. PEG and dextran are chemically distinct crowding agents. Dextran is composed of  $\alpha$ -D-1,6-glycosidic-linked glucose molecules with branching (~5%) occurring at  $\alpha$ -1,3 linkages, while PEG is a H-(O-CH<sub>2</sub>-CH<sub>2</sub>)<sub>n</sub>-OH polymer. Since both polymers are chemically distinct, it is expected that any differences in the respective enzymatic properties of EF-Tu caused by the two crowders are due to nonspecific interactions occurring. Further, dextran 40 solutions are

much more viscous than PEG 4000 solutions at the same concentrations controlling for any effect caused by a change in viscosity of the solution. Here we used a kinetic approach complemented with molecular dynamics (MD) simulations of EF-Tu•GTP and EF-Tu•GDP to ask whether volume exclusion compacts functionally relevant regions of EF-Tu, so that the speed of guanine nucleotide association or dissociation is altered.

## **Materials and Methods**

**Buffers:** Buffer A: 25mM Tris-HCl (Fisher Scientific), pH 7.5, 50mM NH<sub>4</sub>Cl (BioBasic), and 10mM EDTA (BioBasic). Buffer B: 25mM Tris-HCl, pH 7.5, and 50mM NH<sub>4</sub>Cl. Buffer C: 50mM Tris-HCl, pH 7.5, 70mM NH<sub>4</sub>Cl, 30mM KCl (BioBasic), and 7mM MgCl<sub>2</sub> (Biobasic).

**Molecular dynamics simulations. Model construction:** The same method outlined in Wieden *et al.* (2010) was followed to generate the initial structures. Briefly, a homology model was generated using ExPASy Proteomics Server (<http://www.expasy.org>) for the initial structure of the EF-Tu•GTP bound conformation. The homology model was based on the X-ray crystal structure of EF-Tu•GDPNP from *T. aquaticus* (PDB ID 1EFT) (93). The reference structure used for the MD simulation of EF-Tu•GDP was based on the X-ray crystal structure of EF-Tu•GDP from *E. coli* (PDB ID 1EFC) (11). Seven N-terminal amino acids that were missing from the EF-Tu•GDP crystal structure were substituted with conformations identical to those in the EF-Tu•GTP bound conformation. The psfgen package in VMD (100) was used to add hydrogen atoms to both models and to protonate histidine side chains at the  $\xi$ -nitrogen. Both structures were solvated with a water box at least 10 Å away from the protein each direction using the VMD SOLVATE package. The



system was relaxed by minimizing the positions of the water molecules then the protein and ligand ions. This was done for two iterative rounds. The AUTOIONIZE package in VMD was used to add sodium ions (N=7) into random positions to neutralize the total charge (100). A final minimization was done using NAMD until there was no change in total energy for 1000 steps (101). *Simulation parameters:* Simulations with both the EF-Tu•GTP complex and EF-Tu•GDP complex were formed using NAMD (102) with the CHARMM 22 force field for proteins (103) and CHARMM 27 force field for nucleic acids (104). Periodic cell boundary conditions were used. The temperature, number of atoms and pressure were held constant during our simulation. The temperature used for the entire simulation was 300 K. The step size used for saving each frame was 0.5 ps. The simulation was run for a total of 40 ns. Every 10 000<sup>th</sup> frame was used for analysis. Before analysis the each frame in the simulation was fit to the first frame with Carma and water and sodium molecules were removed (105). The root mean square fluctuation (RMSF) of the C<sub>α</sub> of each amino acid was calculated with script written in house and VMD.

***Expression and purification of EF-Tu.*** EF-Tu was expressed and purified to homogeneity as described in (15, 106). To prevent EF-Ts co-purification all steps contained GDP. EF-Tu concentration was determined with the extinction coefficient of 32,900 M<sup>-1</sup>cm<sup>-1</sup> at a wavelength of 280nm. Extinction coefficient was determined with ProtParam (83). Protein purity was assessed by 12% SDS PAGE stained with Coomassie Brilliant Blue.

***Preparation of nucleotide free EF-Tu.*** Nucleotide free EF-Tu was prepared as described

in (15, 106). EF-Tu•GDP was incubated with Buffer A at 37°C for 30min to chelate the magnesium ion and promote the dissociation of GDP. Then EF-Tu and GDP were separated on a Superdex 75 (GE healthcare) size exclusion column in Buffer B. Fractions containing EF-Tu were collected and the concentration was quantified with the extinction coefficient of  $32,900\text{M}^{-1}\text{cm}^{-1}$  at a wavelength of 280nm. The EF-Tu extinction coefficient was determined with ProtParam (83). EF-Tu was diluted with Buffer C prior to all experiments. Rapid kinetic assays were done on the same day as the preparations of nucleotide free EF-Tu.

***Rapid Kinetics Measurements.*** For solutions containing dextran 40 (*Leuconostoc spp.*  $M_r \sim 40,000$ , Sigma-Aldrich) or PEG 4000 (BioUltra 4,000,  $M_r$  3500-4500, Sigma-Aldrich, 50% (w/v) solutions were prepared in Buffer C and the pH was adjusted to 7.5 at room temperature. Dextran 40 is very viscous at 50% (w/v); therefore, we used the density (1.1929 g/mL) of dextran at 50% (w/v) to measure out the mass of dextran corresponding to the concentration used to the nearest 1mg. PEG 4000 50% (w/v) was pipetted into solutions to reach the desired concentration. Glucose (BioBasic) solutions were prepared as crowding solutions. For all stopped-flow experiments both syringes were filled to the same concentration of crowding agent. The fluorescence stopped-flow apparatus (KinTek SF-2004) was used to determine elementary rate constants of nucleotide binding as described in (6). Fluorescence energy transfer from the single tryptophan ( $\lambda_{\text{ex}} = 280\text{nm}$ ) in EF-Tu to the mant-GTP or mant-GDP (Molecular Probes, Eugene, OR) was detected after passing through an LG-400-F filter (Newport Filters). Software used to fit a one exponential function (equation 1) to the observed fluorescent trace was TableCurve (Jandel Scientific). Prism (GraphPad Software) software was used

generate all plots and fit a linear function to data.

Nucleotide association rates were determined under pseudo first order conditions by titrating mant-GTP/GDP against a constant concentration of nucleotide free EF-Tu (0.3-0.5 $\mu$ M). The apparent rate constant for each mant concentration was determined by fitting a one exponential function (Equation 1) to each fluorescence time course. The association rate constant was determined by plotting the apparent rate with respect to nucleotide concentration.

Dissociation rate constants were determined by forming an EF-Tu•mant-GTP/GDP complex with 0.3 $\mu$ M EF-Tu and 3 $\mu$ M mant nucleotide. Then EF-Tu•mant-GTP/GDP was chased with 30 $\mu$ M of unlabeled nucleotide. The dissociation rate constant was determined by fitting each time course to a one exponential function (equation 1).

## **Results**

### ***Macromolecular crowding modifies the rate of GTP association to EF-Tu.***

The association rate of mant-GTP and mant-GDP was determined under pre-steady state and pseudo first order conditions. EF-Tu contains a single tryptophan residue (Trp 184 *E. coli* numbering) proximal to the binding pocket. When excited at a wavelength of 280nm, this tryptophan can transfer energy to a fluorophore, such as mant, if the fluorophore is near the binding pocket. The emission of this fluorophore can be observed after passing through a long wavelength filter. Each observed fluorescence trace was fit to a single exponential function to determine each apparent rate. Since the observed association rate is dependent on the nucleotide concentration, increasing concentrations of excess mant labeled nucleotides were rapidly mixed with a constant

concentration of nucleotide-free EF-Tu. This was repeated at different concentrations of the respective crowding agent (Figure 16 and Figure 18). For GTP association, under all conditions tested the concentration dependence of the  $k_{app}$  with respect to the nucleotide concentration is always linear; therefore, a linear function was fit to the data to determine the association rate ( $k_{on}$ ) for each condition (Figure 16). The association rate with respect to crowder concentration is plotted in Figure 17. A linear trend was observed between the association rate and the concentration of dextran 40. As the concentration of dextran increased the rate of GTP association decreased. Under dilute conditions, the association rate was observed to be  $(4.0 \pm 0.1) \times 10^5 \text{ M}^{-1}\text{s}^{-1}$ . This association rate agrees with the reported value of  $(5 \pm 1) \times 10^5 \text{ M}^{-1}\text{s}^{-1}$  (6). Under dextran-crowded conditions, the rate gradually decreased to  $(2.4 \pm 0.3) \times 10^5 \text{ M}^{-1}\text{s}^{-1}$  of 25% (w/v) dextran concentration. PEG 4000 also reduced the association rate of GTP; however, the concentration dependence was more complex deviating from linear behavior. At 25% (w/v) PEG 4000, the association rate was reduced to  $(0.9 \pm 0.1) \times 10^5 \text{ M}^{-1}\text{s}^{-1}$ . Similarly, 25% glucose reduced the rate to  $(1.3 \pm 0.1) \times 10^5 \text{ M}^{-1}\text{s}^{-1}$ .

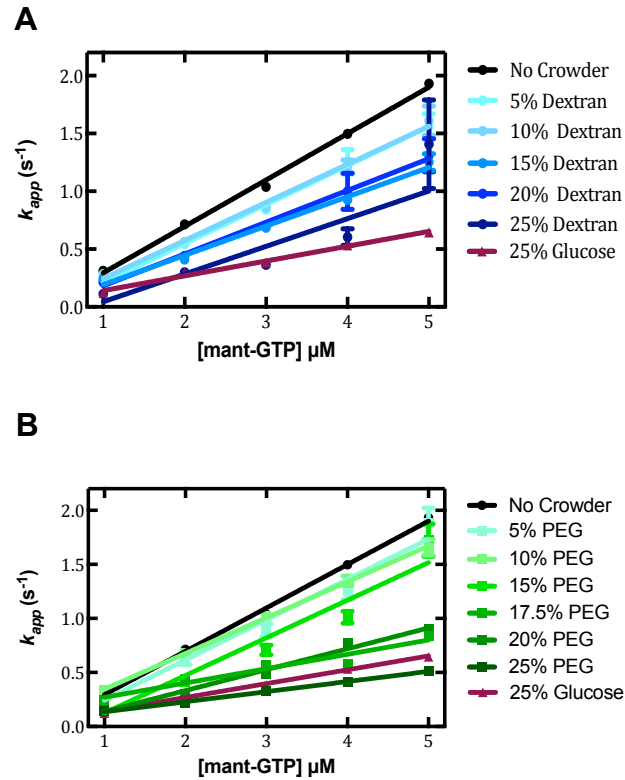


**Figure 16: Effect of molecular crowding on the association rate of GTP.**

The effect of macromolecular crowding induced by either (Panel A) dextran 40 (w/v) or (Panel B) PEG 4000 (w/v) on the apparent association rate of nucleotide free EF-Tu ( $\sim 0.5 \mu M$ ) and mant-GTP nucleotides with respect to the mant-GTP concentration. Time course were gathered by observing the fluorescent energy transfer from the single tryptophan residue in EF-Tu to the mant group, and then time courses were fit to a one exponential function, to determine the  $k_{app}$ . Each point is the average of at least seven time courses at the indicated nucleotide concentration, and the error bars are the standard error.

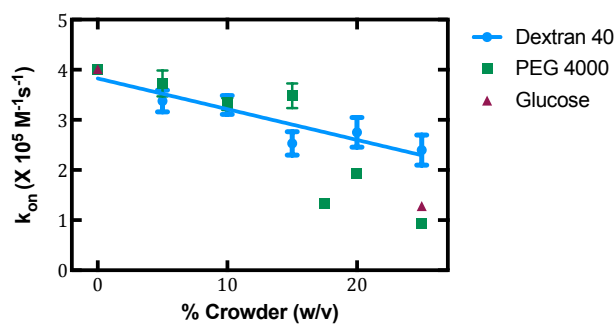


**Figure 17: Effect of molecular crowding on the association rate of GTP.**

Effect of increasing the extent of macromolecular crowding induced by either dextran 40 or PEG 40 on the rate constant of nucleotide-free EF-Tu and mant-GTP associating. Each point is the slope of the  $k_{app}$  with respect to nucleotide concentration (Figure 16) determined at each crowder concentration, and error bars are the error from the linear fit used to calculate the slope.

The association rate constant between EF-Tu and GDP is an order of magnitude greater than the association rate constant for GTP (6). Therefore, if the viscosity of the crowded solutions had decreased the rate constant of GTP association to EF-Tu, we should observe a decrease in the rate of GDP association as crowding increases. Further, the rate should be more affected for GDP association than GTP association, because the GDP association rate constant is an order of magnitude greater than the GTP association rate constant (6). Under each condition tested, the apparent rate constant exhibits a linear dependence with respect to mant-GDP concentration (Figure 18). The association rate constant was determined, and is plotted with respect to crowder concentration in Figure 19. We did not observe a decrease in the association rate as crowder concentration increased. Instead the association rate of GDP to EF-Tu was not significantly affected by dextran 40 up to concentrations of 25% (w/v). Low concentrations of PEG 4000 increased the rate of GDP association until a concentration of 15% (w/v) was reached. At 15% (w/v) PEG 4000, the rate constant of GDP association returned to  $(1.9 \pm 0.3) \times 10^6 \text{ M}^{-1}\text{s}^{-1}$ , which is similar to the rate constant of  $(1.7 \pm 0.1) \times 10^6 \text{ M}^{-1}\text{s}^{-1}$  in dilute solution (6). In concentrations of 20% (w/v) and 25% (w/v) PEG the association rate constant remained similar to the rate constant in dilute solution. In contrast to macromolecular crowding agents, glucose decrease the rate of GDP association to  $(0.6 \pm 0.1) \times 10^5 \text{ M}^{-1}\text{s}^{-1}$ . This decrease in association rate is expected if glucose packed around the structure of EF-Tu, and slowed conformational changes (7, 107, 108).

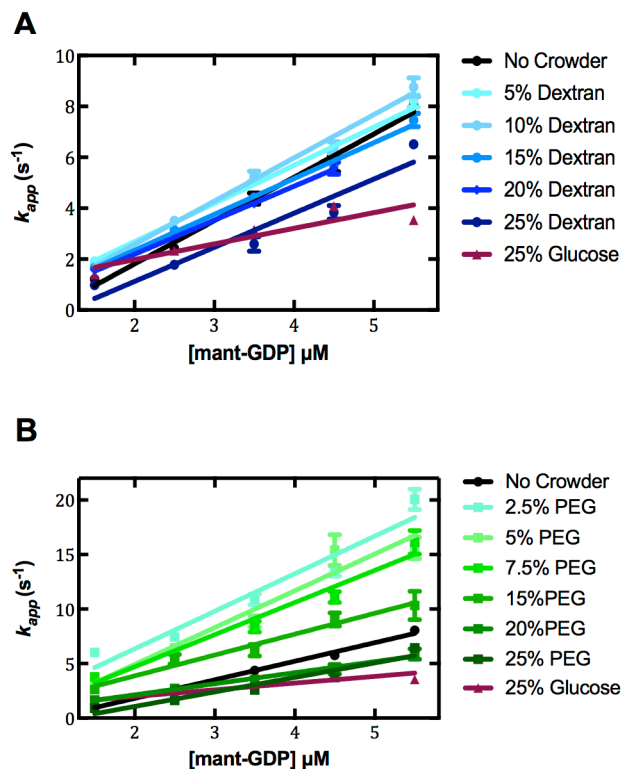


**Figure 18: Effect of molecular crowding on the association rate of GDP.**

The effect of macromolecular crowding induced by either (Panel A) dextran 40 (w/v) or (Panel B) PEG 40 (w/v) on the apparent rate of mant-GDP association to nucleotide free EF-Tu ( $\sim 0.5 \mu\text{M}$ ) with respect to the nucleotide concentration. Time courses were recorded by observing the fluorescent energy transfer from the single tryptophan in EF-Tu to the mant group, and each time course was fit to a one exponential function to determine the  $k_{app}$ . Each point on the graph represents an average of at least seven time courses at the indicated nucleotide concentration, and the error bars are the standard error.



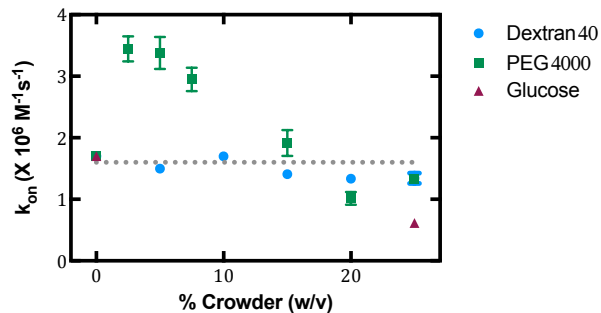


**Figure 19: Effect of molecular crowding on the association rate of GDP.**

The effect of increasing macromolecular crowding induced by either dextran 40 or PEG 40 on the rate constant of mant-GDP associating to EF-Tu. The rate constant was determined from the slope of the  $k_{app}$  with respect to nucleotide concentration (Figure 18). The grey dashed line represents the theoretical fit of crowding having no effect on GDP association. The error bars are the error of the linear fit used to determine the slope.

***Macromolecular crowding decreases the rate of GDP dissociation from EF-Tu.***

For EF-Tu, nucleotide dissociation is very slow compared to nucleotide association, and as such dissociation is rate limiting. Macromolecular crowding was not expected to decrease the rate constant of GTP dissociation from EF-Tu, because switch I is likely flexible in both the apo and GTP bound form. However, crowding is expected to decrease the rate constant of GDP dissociation from EF-Tu, because switch I will go from a rigid structure to a flexible one (52). If crowders increased the rate constant of nucleotide dissociation it would be concerning, because this could mean that the crowding agents are negatively impacting the stability of the structure through nonspecific chemical interactions (53). Nucleotide dissociation from EF-Tu was performed as a chase experiment. This involved rapidly mixing EF-Tu•mant-GTP/GDP with a large excess of unlabeled nucleotide. Since nucleotide dissociation is a first order reaction and the rebinding of unlabeled nucleotides occurs rapidly under these conditions, the apparent rate of mant-nucleotide dissociation is the rate constant of dissociation (6). Each observed fluorescence trace for nucleotide dissociation was fit to a single exponential function to obtain the dissociation rate constant. Neither crowding agent strongly affected the dissociation rate constant of GTP from EF-Tu (Figure 20). In dilute solution and under crowded conditions the rate constants agree with the literature reported value of  $(0.03 \pm 0.01) \text{ s}^{-1}$  (6). In contrast to crowding agents, 15% glucose decreased the dissociation rate constant from  $(0.016 \pm 0.001) \text{ s}^{-1}$  to  $(0.008 \pm 0.002) \text{ s}^{-1}$ .

For GDP dissociation, dextran 40 and PEG 4000 had a similar affect on the rate constant (Figure 21). Both crowding agents decreased the rate constant of GDP dissociation, in a linear fashion. The rate constant of dissociation in dilute solution was

$(0.0014 \pm 0.0001) \text{ s}^{-1}$  and was in agreement with the value reported in literature (6). In crowded solutions of 15% (w/v) dextran the rate constant decreased to  $(0.0005 \pm 0.0001) \text{ s}^{-1}$  and to  $(0.0008 \pm 0.0001) \text{ s}^{-1}$  in solutions crowded with 15% (w/v) PEG 4000. Similarly, 15% (w/v) glucose decreased the rate of GDP dissociation to  $(0.0009 \pm 0.0005) \text{ s}^{-1}$ ; however, this decrease in the rate constant is likely the result of a different mechanism than volume exclusion (4, 7, 107, 108), because the rate constant of GTP dissociation also decreased in glucose, but did not decrease in crowded solutions.

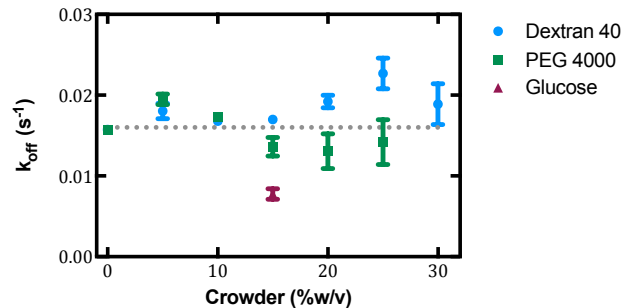


**Figure 20: Effect of macromolecular crowding on the dissociation rate constant of GTP.**

Effect of increased macromolecular crowding induced by either dextran 40 or PEG 40 on the dissociation rate constant of EF-Tu dissociating from mant-GTP. The dissociation rate constant of EF-Tu and mant-GTP was determined by following the fluorescence energy transfer from the single tryptophan in EF-Tu to the mant group, and fitting each time course to a single exponential function. The grey dashed line represents the theoretical fit of crowding having no effect on the dissociation rate constant of GTP. Each point represents the average of at least 11 time courses, and the error bars are the standard error.

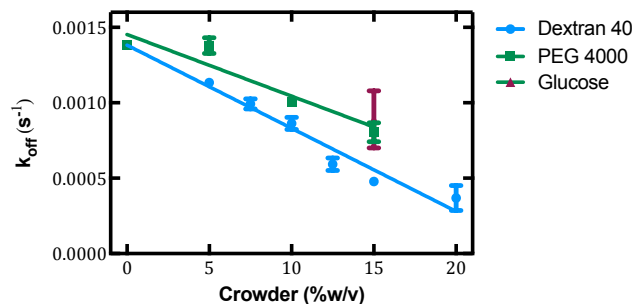


**Figure 21: Effect of macromolecular crowding on the dissociation rate constant of GDP.**

The effect of increasing macromolecular crowding by dextran 40 or PEG 40 on the dissociation rate constant of EF-Tu and mant-GDP. The dissociation rate constant was determined from the time course of fluorescent energy transfer from the single tryptophan in EF-Tu to the mant group by fitting each time course to a single exponential function. Each point on the graph represents the average of at least six time courses, and the error bars are the standard error.

### ***Differences in flexibility between the GTP and GDP conformation of EF-Tu.***

The function of EF-Tu is modulated by its nucleotide-bound state because of the difference in conformation. To predict the effects of macromolecular crowding on the GTP- and GDP-bound states, we performed molecular dynamics (MD) simulations and monitored the root mean square fluctuation (RMSF) of the  $C_{\alpha}$  in each amino acid (Figure 23). To color each amino acid by relative flexibility, the protein data bank (pdb) file was modified to include the RMSF value for each  $C_{\alpha}$  (Figure 22). Overall, EF-Tu•GDP had a higher RMSF value, but the EF-Tu•GTP structure had more regions that were flexible compared to the flexibility of the entire structure. Flexible regions with respect to the relative RMSF value present in each conformation are listed in Table 4. It is of particular interest that switch I is flexible in the GTP-bound simulation, but not in the GDP simulation. Switch I and switch II regions participate in the drastic conformational change from the GTP state to the GDP state (11, 93). Specifically, during the conformational change from the GTP bound state to the GDP-bound state, the structure of switch I changes from two short  $\alpha$  helices into two  $\beta$  strands (11, 93). Along with switch I and II regions reorganizing, domain I rotates by  $90^{\circ}$  compared to domain II and domain III, which changes the interactions between domain I and domain II in the two structures (11). In addition to switch I being more flexible in the GTP conformation, the loop regions are much more flexible in the GTP conformation compared to the rest of the structure (Figure 22). In the EF-Tu•GTP simulation, all the  $\beta$  sheets in domain II and domain III are rigid while almost all the loops are flexible. In the EF-Tu•GDP, simulation only a handful of loops are flexible compared to the  $\beta$  sheets. The conformation of apo EF-Tu is unknown, but since nucleotide-free EF-Tu is very unstable (109), apo EF-Tu

must have a distinct conformation from either nucleotide bound form, and most likely the switch I motif is disordered. Macromolecular crowding compacts flexible regions (5, 55) and has been suggested to reduce conformational sampling (107, 108); therefore, the conformational change of switch I required for nucleotide binding could be impaired. It would be expected that the conformational change from apo to GTP bound would be more affected, because switch I region remains flexible, whereas switch I is more rigid in the GDP conformation. In contrast to crowding agents, the osmolyte glucose is not expected to induce an excluded volume effect (4). Instead osmolytes like glucose tend to decrease the surface area of the protein, because they are preferentially excluded from the protein backbone (7, 110). In addition osmolytes hinder conformational changes that expose binding interfaces (7, 111). Glucose is expected to hinder conformational changes associated with nucleotide association and dissociation similarly, because of the domain reorientation in EF-Tu required for nucleotide binding (11, 93).

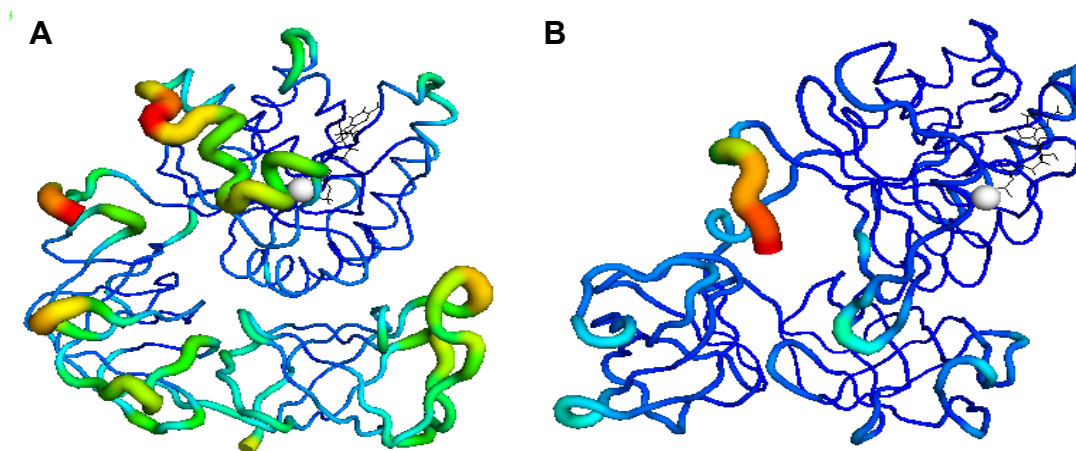


**Figure 22: Cartoon representation of EF-Tu in the GTP and GDP bound states.**

Cartoon representation of EF-Tu in the (A) GTP- and (B) GDP-bound states. EF-Tu is colored by relative RMSF values obtained from 40 ns MD simulations. The more relative flexibility there is in a region, the thicker it is, and it is colored red. Relatively rigid regions are thin and blue.



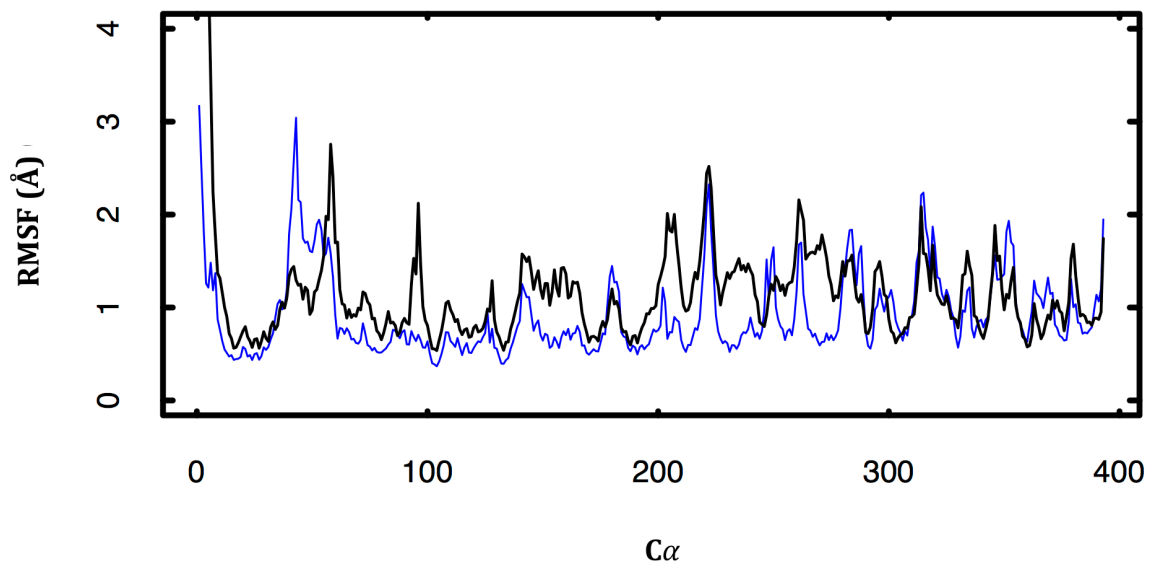


**Figure 23: RMSF with respect to the  $C_{\alpha}$  of each amino acid for 40 ns MD simulations.**

EF-Tu in the GTP state is blue and the GDP state is black.

**Table 4:** Regions in the GTP and GDP conformation of EF-Tu that are more flexible compared to the entire structure during 40 ns molecular dynamics simulations. These are the same regions that are flexible in Figures 22 and Figure 23.

<b>GTP Conformation</b>		<b>GDP Conformation</b>	
<b>Domain</b>	<b>Structure</b>	<b>Domain</b>	<b>Structure</b>
I	N-terminus (Ser1 - Lys9)	I	N terminus (Ser1 - Arg7)
I	Switch I (Val34 - ILE60)	I	Loop (Ala57 - Ile60)
I	Loop (Asn135 - Glu143)	I and II	Loop (Tyr198 - Leu211)
I	Loop (Leu178 - Ala182)	II	Loop (Ser219 - Thr225)
I and II	Loop (Tyr198 - Leu211)	II	Loop (Met260 - Lys263)
II	Loop (Ser219 - Thr225)	III	Loop (Arg269 - Asn273)
II	Loop (Lys237 - Glu241)	III	Loop (Tyr310 - Gln329)
II	Loop (Met260 - Lys263)	III	C- terminus (Ser393)
II	Loop (Leu278 - Val291)		
II and III	Loop (Ala293 - Lys299)		
III	Loop (Ile310 - Gln329)		
III	Loop (Phe332 - Thr335)		
III	Loop (Glu342 - Asn355)		
III	Loop (Met368 - Arg373)		
III	Loop (Glu378 - Arg381)		
III	C-terminus (Ala389 - Ser393)		

## Discussion

Macromolecular crowding affects the entropy of the system through volume exclusion. Volume exclusion decreases the entropy of the system so that compact states that occupy less volume are favored (52). It has also been shown that both the native states (5, 54, 55) and unfolded states are compacted by crowding (112, 113). Particularly, flexible regions within a protein are compressed (5, 54, 55). Osmolytes such as glucose are not typically recognized as inducing macromolecular crowding effects, because they do not create steric repulsion through volume exclusion (107, 108, 114). Instead, glucose is excluded from the protein surface, and increases burial of the protein backbone (7, 107). This causes compaction and stabilization of the protein resulting in decreased conformational sampling (4, 108). Here we used MD simulations to predict flexible regions within EF-Tu in the GTP- and GDP-bound states. We found that while the GDP state had an overall higher RMSF, the GTP state had more distinct flexible regions; particularly in switch I involved in the large-scale structural transition between the GTP and GDP state (11, 93), was found to be flexible in the GTP simulation and not the GDP simulation (Figure 22). Based on the simulations, we reasoned crowding agents would compact EF-Tu in such a way that would reduce the flexibility observed in the switch I region of the GTP state. This in turn would result in the GDP conformation being favored over the GTP conformation. In addition to crowding affecting the flexibility, macromolecular crowding would affect the entropy of binding (52). GTP binding to EF-Tu is entropically favored compared to GDP (*personal communication*), and crowders would diminish this effect. To show this was an effect of macromolecular crowding we used two chemically distinct crowding agents: dextran 40 and PEG 4000. Both crowding

agents induced a similar effect on the nucleotide binding properties of EF-Tu, suggesting the observed effects were due to volume exclusion and not nonspecific chemical interactions. As the concentration of either crowding agent increased to 25% (w/v) the rate of GTP association decreased by about 2 fold (Figure 17), while the rate of GDP association was not affected (Figure 19). For dissociation, neither crowder affected the rate of GTP dissociation (Figure 20); however, crowding at 15% (w/v) reduced the rate of GDP dissociation by about 2 fold (Figure 21). Overall the affinity of EF-Tu decreased by about 4 fold for GTP in 25% (v/w) crowded solutions, while increasing by 3 fold for GDP in 15% (v/w) crowded solutions.

The osmolyte glucose did not induce the same affect as crowding agents. Glucose slowed both the association rates and dissociation rates of guanine nucleotide similarly. This effect would be expected if glucose hindered conformational changes that exposed buried surfaces (7). EF-Tu undergoes a significant conformational rearrangement as a result of nucleotide binding, which exposes buried surfaces (11, 93). Osmolytes have been previously observed to exert effects that differ from polymer solutions used to induce macromolecular crowding (4).

Although the overall effects of dextran 40 and PEG 4000 were similar with respect to the nucleotide binding properties of EF-Tu only dextran exhibited linear behavior on both nucleotide association rate (Figure 17 and 5) and nucleotide dissociation rate (Figure 20 and 7). The effect of PEG 4000 on the association rate of GTP to EF-Tu was complex and could not be fit with a linear equation (Figure 17). When the PEG 4000 concentration was under 10% (w/v), the rate of GDP association increased with respect to the absence of PEG 4000 (Figure 19). The effects of PEG 4000 in the low concentration

regime can be explained by nonspecific chemical interactions. Nonspecific chemical interactions between crowding agents and the macromolecule under study have been documented to occur under low crowder concentrations, and under higher crowder concentrations these interactions have been masked by the larger effect of volume exclusion (97).

We do not expect the change in viscosity from the soluble polymers to significantly affect the rate of nucleotide association. Nucleotide association rates are not in the regime of diffusion controlled reactions, which have rates in the  $10^8 \text{ M}^{-1} \text{ s}^{-1}$  range (6). Macromolecular crowding slows reactions that are diffusion limited, but increase reactions that are transition state limited and favor a more compacted transition state (4, 52). If the change in viscosity did impact nucleotide association rate, we would expect that both GTP and GDP association rates would be reduced. Instead we observed that only the rate of GTP association was decreased (Figure 17). The faster rate of GDP association rate was not affected by high concentrations of dextran 40 or PEG 4000 (figure 19). Further, the rate of GDP association was increased in low concentrations of PEG 4000. The viscosities of dextran 40 and PEG 4000 solution were different, because of the size difference of the two polymers. Dextran 40 is approximately an order of magnitude larger than PEG 4000; therefore, we would expect dextran 40 to slow rates more than PEG 4000 if viscosity had a significant effect. However, we did not observe dextran 40 slowing rates more than PEG 4000.

The effect of macromolecular crowding on EF-Tu has biological implications. Since the affinity for GTP is reduced and affinity for GDP increases as macromolecular crowding increases, EF-Tu would spend more time in the inactive state under crowded

conditions compared to dilute conditions, which could reduce the overall speed of translation. It was also observed that nonspecific chemical interactions could further increase the affinity of EF-Tu for GDP (Figure 19). The contents of the cell are not inert, so macromolecular crowding within the cell is expected to result in some nonspecific chemical interactions (115). Of course in the cell, EF-Tu interacts with EF-Ts, which increase the rate of nucleotide dissociation (6). Scaled particle theory has suggested that macromolecular crowding should increase the association rate between macromolecules by orders magnitude at physiological volume occupancy (116). However, *in vitro* and *in vivo* studies have only observed modest increases, no effects, or reduced association rates and stability of dimers in crowded solutions compared dilute buffer (115). The effects of macromolecular crowding on the interaction of EF-Tu and EF-Ts depend on the size and shape of each protein, the shape and size of the dimer, and the shape and size of the crowders. Recently, it has been observed that macromolecular crowding limits translation, because of the slowed diffusion of the EF-Tu•GTP•aa-tRNA complex to the ribosome (117). The slowed diffusion of the EF-Tu•GTP•aa-tRNA complex to the ribosome is the dominant effect in the cell and it is predicted to limit the speed of translation and lead to a reduced growth rate (117). In addition to volume exclusion effects, macromolecular crowding induces confinement (52). Confinement results when macromolecules can no longer diffuse freely. In *E. coli* such condition can occur upon increased osmotic pressure when water freely diffuses out of the cytoplasm and increases crowding. Small metabolites can still freely and evenly diffuse through the cell under these conditions, but larger macromolecules become trapped (118). Confinement has been speculated to be involved in the formation of functional partitions in prokaryotes (119),

such as the specific cellular locations of replication, transcription, and translation machinery within the cell (120). EF-Tu's transition into the GTP was slowed even modestly in the cell, the effects could be amplified over the translation cycle. Given that the average length of a protein is about 300 amino acids in *E. coli* (121), EF-Tu molecules will need to be recycled back to the GTP state at least 300 times in total. For instance, the average speed of translation *in vivo* is ~15 amino acids per second (122). For a protein consisting of 300 amino acids it would take the ribosome ~20 s to translate. From the *in vitro* data the rate constant of GDP dissociation was slowed by an order of magnitude (Figure 21), and the rate constant of GTP association was slowed by a factor of two (Figure 17). If the recycling of EF-Tu was decreased by 25%, it could take ~25 s to translate a protein consisting of 300 amino acids.

## **Conclusion**

We observed distinct effects due to macromolecular crowding induced by dextran 40 and PEG 4000 from those of high concentrations of the osmolyte glucose. We were able to determine that the affinity of GTP is reduced in crowded conditions, because the rate of GTP association is decreased. The affinity of EF-Tu from GDP was increased in crowded solutions, because the rate of GDP dissociation was reduced. Glucose decreased all rates similarly and therefore did not have an effect on nucleotide affinity.

## Chapter 4: Conclusion

### Conclusion of the effect of tetracycline and macromolecular crowding on the function of EF-Tu

EF-Tu was chosen to study the effect of small molecule inhibitors and macromolecular crowding on protein dynamics that contribute to its function. EF-Tu is an ideal protein to investigate protein dynamics because it undergoes a large conformational change from its active GTP bound state to its inactive GDP bound state (11, 12) (Figure 1). Further, the ability of EF-Tu to form complexes with its interaction partners is directed by the nucleotide bound state (23). There are four structurally distinct classes of antibiotics that bind to and alter the dynamics of EF-Tu so that it can no longer perform its function (3, 27, 28). Another class of antibiotics, the tetracyclines, was speculated to interfere with the function of EF-Tu. This prediction was based on the crystal structure of the trypsin modified EF-Tu•GDP•tetracycline complex (14). However, there was no biochemical data to suggest that the function of *E. coli* EF-Tu was impeded by tetracycline. In addition to no biochemical studies investigating the role of tetracycline on *E. coli* EF-Tu, there have been no studies investigating the effect of macromolecular crowding on the dynamics and function of EF-Tu. Determining if tetracycline or macromolecular crowding influence the dynamics of the factor in a manner that affects its function will aid in finding new conformations EF-Tu, which subsequently can be used to find new antibiotic binding pockets. It is known that macromolecular crowding has an affect on protein flexibility (4, 5). A property that plays a large role in ligand recognition and binding (123). If macromolecular crowding or tetracycline affects the flexibility of EF-Tu the population distribution of EF-Tu molecules in different side chain



conformations, loop and secondary structure rearrangements, and domain arrangements may be altered in a manner that affects ligand binding by stabilizing specific active or inactive conformations of the protein. Further, antibiotics that are known to affect EF-Tu could have altered function *in vivo* if macromolecular crowding affects the population distribution of EF-Tu in different conformations. In this thesis, I addressed two questions related to the dynamics and function of EF-Tu. First, I have successfully demonstrated that binding of tetracycline to EF-Tu does not affect the dynamics of EF-Tu contributing to its cellular function. Secondly, it was determined that macromolecular crowding induced by the synthetic polymers dextran 40 and PEG 4000 does affect the dynamics of nucleotide binding in EF-Tu.

Tetracycline is able to bind trypsin-modified EF-Tu (Figure 5), which does not contain the switch I region of EF-Tu (14); however, tetracycline does not influence the dynamics of intact EF-Tu that contribute to the function of the protein. Most likely, the interaction between tetracycline and EF-Tu is mediated by the magnesium ion and the interaction is weak (124). Also unlike the other classes of antibiotics that are known to effect EF-Tu, tetracycline does not widen any domain interfaces or reorient any domains in EF-Tu. Combining the biochemical experiments presented in this thesis and the crystal structure of the trypsin modified EF-Tu•GDP•tetracycline complex (14), it is unlikely that tetracycline induces a new conformation in EF-Tu or has any affect on the distribution of EF-Tu conformations. Further, using the EF-Tu•GDP•tetracycline complex as a model for the discovery of new small molecule inhibitors that affect GTPase and ATPase with a similar binding pocket should be dismissed.

The use of the synthetic crowding agents dextran 40 and PEG 4000 to study the effect of macromolecular crowding on EF-Tu suggests that protein dynamics should be studied in more cellular-like environment. It was observed that both dextran 40 and PEG 4000 had the same effect on the intrinsic nucleotide binding properties of EF-Tu. Both synthetic polymers reduce the rate constant of GTP association to EF-Tu (Figure 17), but did not affect the rate constant of GDP association (Figure 19), and both polymers decreased the rate constant of GDP dissociation (Figure 20), but did not affect GTP dissociation (Figure 21). Since the binding of guanine nucleotides to EF-Tu is not diffusion controlled reaction, but rather controlled by a conformational change (6), macromolecular crowding is influencing the dynamics in EF-Tu by modulating the speed with which this conformation change occurs. In contrast to macromolecular crowding agents, the osmolyte glucose decreased all rates by likely preventing conformational changes which exposed new surfaces in EF-Tu, consistent with the notion that sugar osmolytes induce burial of the protein backbone (7). The results in this thesis show distinct effects between macromolecular crowding and osmolyte effects. This is consistent with macromolecular crowding acting through volume exclusion and limiting the radius of gyration of proteins and other macromolecules (8, 52).

#### **Future directions for macromolecular crowding studies involving EF-Tu**

Continuing on the effect of macromolecular crowding on the nucleotide binding properties of EF-Tu, it would be interesting to study how macromolecular crowding tunes the speed of conformational changes in EF-Tu. One way to approach this would be to study the how the different populations of EF-Tu change in a crowded environment using intramolecular fluorescence resonance energy transfer (FRET). Using a

spectrofluorometer equilibrium ensemble measurement, FRET could be used as a spectroscopic ruler to determine if increased crowding changes the distance between regions in EF-Tu. This technique has been used for other crowding studies (125). These same fluorescently labeled EF-Tu molecules could also be used in a single molecule setup. The single molecule FRET results would give information on how long EF-Tu remained in particular conformations and the population distribution of conformations. This information could be critical in setting up *in vitro* drug screening platforms that consider the crowded cellular-like environment.

Either the current stopped-flow setup described in this thesis (*chapter 3 methods section*) or a single molecular FRET setup could be used to determine if antibiotics known to affect EF-Tu's function, kirromycin, enacyloxin, pulvomycin and GE2270 A, have the same effect under dilute and crowded conditions. It would be particularly interesting to study how crowding influences kirromycin's ability to induce a more GTP like state in EF-Tu (2). Kirromycin has been observed to increase the flexibility of switch I in EF-Tu, and kirromycin has been shown to increase the affinity of GTP to EF-Tu (2). Based on the data in this thesis it is predicted that switch I is less flexible under crowded conditions (Figure 22 and Table 4). A reasonable hypothesis would be that macromolecular crowding reduces the flexibility of switch I in the presence of kirromycin, which would decrease the observed increase in GTP affinity in the presence of kirromycin.

In addition to studying spontaneous nucleotide exchange in EF-Tu, the more *in vivo* EF-Ts catalyzed nucleotide exchange in EF-Tu should be studied under crowded conditions. EF-Ts is needed to maintain *in vivo* translation rates (6), and it is unknown how

macromolecular crowding would affect the diffusion or conformation of EF-Ts and the EF-Tu•EF-Ts complex in the GDP, GTP or apo state. The interaction of EF-Tu and EF-Ts in crowding agents could be studied through similar stopped-flow experiments presented in this thesis (Figure 12). The structures of the EF-Tu•GDP•EF-Ts, EF-Tu•GTP•EF-Ts, and EF-Tu•EF-Ts could be investigated under crowded conditions using small angle X-ray scattering to provide evidence that crowding induces a more compact conformation. It would also be interesting to determine which regions in the different nucleotide bound forms of the EF-Tu•EF-Ts change their flexibility. For instance, the flexibility of the P-loop in EF-Tu is important for nucleotide exchange in EF-Tu (25, 106). It would be interesting to determine if the flexibility of the P-loop is impacted by macromolecular crowding, and how this change in flexibility alters EF-Ts stimulated nucleotide dissociation in EF-Tu. Overall, this will help to address the overarching question: Is molecular crowding a feature of biological function influencing evolution and overall performance of biomolecules?

## References

1. Bennett BD, Kimball EH, Gao M, Osterhout R, Van Dien SJ, Rabinowitz JD. Absolute metabolite concentrations and implied enzyme active site occupancy in *Escherichia coli*. *Nature Chemical Biology*. 2009;5(8):593-9.
2. Vogeley L, Palm GJ, Mesters JR, Hilgenfeld R. Conformational change of elongation factor Tu (EF-Tu) induced by antibiotic binding - Crystal structure of the complex between EF-Tu•GDP and aurodox. *Journal of Biological Chemistry*. 2001;276(20):17149-55.
3. Parmeggiani A, Krab IM, Watanabe T, Nielsen RC, Dahlberg C, Nyborg J, et al. Enacyloxin IIa pinpoints a binding pocket of elongation factor Tu for development of novel antibiotics. *Journal of Biological Chemistry*. 2006;281(5):2893-900.
4. Hoffman L, Wang X, Sanabria H, Cheung MS, Putkey JA, Waxham MN. Relative Cosolute Size Influences the Kinetics of Protein-Protein Interactions. *Biophysical Journal*. 2015;109(3):510-20.
5. Dhar A, Samiotakis A, Ebbinghaus S, Nienhaus L, Homouz D, Gruebele M, et al. Structure, function, and folding of phosphoglycerate kinase are strongly perturbed by macromolecular crowding. *Proceedings of the National Academy of Sciences*. 2010;107(41):17586-91.
6. Gromadski KB, Wieden H-J, Rodnina MV. Kinetic mechanism of elongation factor Ts-catalyzed nucleotide exchange in elongation factor Tu. *Biochemistry* 2002;41:162-9.
7. Harries D, Rösgen J. A practical guide on how osmolytes modulate macromolecular properties. *Methods in Cell Biology*. 2008;84:679-735.
8. Ellis RJ. Macromolecular crowding: an important but neglected aspect of the intracellular environment. *Current Opinion in Structural Biology*. 2001;11(1):114-9.
9. Kubarenko AV, Sergiev PV, Rodnina MV. GTPases of the translation apparatus. *Molecular Biology*. 2005;39(5):646-60.
10. Vetter IR, Wittinghofer A. The guanine nucleotide-binding switch in three dimensions. *Science (New York, NY)*. 2001;294(5545):1299-304.
11. Song H, Parsons MR, Rowsell S, Leonard G, Phillips SE. Crystal structure of intact elongation factor EF-Tu from *Escherichia coli* in GDP conformation at 2.05 Å resolution. *Journal of Molecular Biology*. 1999;285(3):1245-56.

12. Kjeldgaard M, Nissen P, Thirup S, Nyborg J. The crystal structure of elongation factor EF-Tu from *Thermus aquaticus* in the GTP conformation. *Structure* (London, England : 1993). 1993;1(1):35-50.
13. Berchtold H, Reshetnikova L, Reiser COA, Schirmer NK, Sprinzl M, Hilgenfeld R. Crystal structure of active elongation factor Tu reveals major domain rearrangements. *Nature*. 1993;365(9):126-32.
14. Heffron SE, Mui S, Aorora A, Abel K, Bergmann E, Journak F. Molecular complementarity between tetracycline and the GTPase active site of elongation factor Tu. *Acta Crystallographica Section D-Biological Crystallography*. 2006;62:1392-400.
15. De Laurentiis EI, Mo F, Wieden H-J. Construction of a fully active Cys-less elongation factor Tu: Functional role of conserved cysteine 81. *Biochimica et Biophysica Acta - Proteins and Proteomics*. 2011;1814(5):684-92.
16. Kothe U, Wieden HJ, Mohr D, Rodnina MV. Interaction of helix D of elongation factor Tu with helices 4 and 5 of protein L7/12 on the ribosome. *Journal of Molecular Biology*. 2004;336(5):1011-21.
17. Diaconu M, Kothe U, Schlunzen F, Fischer N, Harms JM, Tonevitsky AG, et al. Structural basis for the function of the ribosomal L7/12 stalk in factor binding and GTPase activation. *Cell*. 2005;121(7):991-1004.
18. Rodnina MV, Pape T, Fricke R, Kuhn L, Wintermeyer W. Initial binding of the elongation factor Tu-GTP-aminoacyl-tRNA complex preceding codon recognition on the ribosome. *Journal of Biological Chemistry*. 1996;271(2):646-52.
19. Kothe U, Rodnina MV. Codon Reading by tRNA<sup>Ala</sup> with Modified Uridine in the Wobble Position. *Molecular Cell*. 2007;25(1):167-74.
20. Pape T, Wintermeyer W, Rodnina MV. Complete kinetic mechanism of elongation factor Tu-dependent binding of aminoacyl-tRNA to the A site of the E.coli ribosome. *The European Molecular Biology Organization Journal*. 1998;17(24):7490-7.
21. Zeidler W, Egle C, Ribeiro S, Wagner A, Katunin V, Kreutzer R, et al. Site-directed mutagenesis of *Thermus thermophilus* elongation factor Tu. Replacement of His85, Asp81 and Arg300. *European Journal of Biochemistry / Federation of European Biochemical Societies*. 1995;229(3):596-604.
22. Fasano O, De Vendittis E, Parmeggiani A. Hydrolysis of GTP by elongation factor Tu can be induced by monovalent cations in the absence of other effectors. *The Journal of Biological Chemistry*. 1982;257(6):3145-50.

23. Kothe U, Rodnina MV. Delayed release of inorganic phosphate from elongation factor Tu following GTP hydrolysis on the ribosome. *Biochemistry*. 2006;45(42):12767-74.
24. Song H, Parsons MR, Rowsell S, Leonard G, Phillips SE. Crystal structure of intact elongation factor EF-Tu from *Escherichia coli* in GDP conformation at 2.05 Å resolution. *Journal of Molecular Biology*. 1999;285(3):1245-56.
25. Mercier E, Girodat D, Wieden H-J. A conserved P-loop anchor limits the structural dynamics that mediate nucleotide dissociation in EF-Tu. *Scientific Reports*. 2015;5:7677.
26. Rodnina MV, Fischer N, Maracci C, Stark H. Ribosome dynamics during decoding. *Philosophical Transactions of the Royal Society B: Biological Sciences*. 2017;372(1716).
27. Parmeggiani A, Krab IM, Okamura S, Nielsen RC, Nyborg J, Nissen P. Structural basis of the action of pulvomycin and GE2270 A on elongation factor Tu. *Biochemistry*. 2006;45(22):6846-57.
28. Parmeggiani A, Nissen P. Elongation factor Tu-targeted antibiotics: Four different structures, two mechanisms of action. *Federation of European Biochemical Societies Letters*. 2006;580(19):4576-81.
29. Wilson DN. The A-Z of bacterial translation inhibitors. *Critical Reviews in Biochemistry and Molecular Biology*. 2009;44(6):393-433.
30. Lamberti A, Martucci NM, Ruggiero I, Arcari P, Masullo M. Interaction between the antibiotic tetracycline and the elongation factor 1alpha from the archaeon *Sulfolobus solfataricus*. *Chemical Biology & Drug Design*. 2011;78(2):260-8.
31. Gordon J. Hydrolysis of guanosine 5'-triphosphate associated with binding of aminoacyl transfer ribonucleic acid to ribosomes. *The Journal of Biological Chemistry*. 1969;244(20):5680-6.
32. Blanchard SC, Gonzalez RL, Kim HD, Chu S, Puglisi JD. tRNA selection and kinetic proofreading in translation. *Nature Structural & Molecular Biology*. 2004;11(10):1008-14.
33. Chopra I, Roberts M. Tetracycline antibiotics: mode of action, applications, molecular biology, and epidemiology of bacterial resistance. *Microbiology and Molecular Biology Reviews*. 2001;65(2):232-60.

34. Brodersen DE, Clemons WM, Jr., Carter AP, Morgan-Warren RJ, Wimberly BT, Ramakrishnan V. The structural basis for the action of the antibiotics tetracycline, pactamycin, and hygromycin B on the 30S ribosomal subunit. *Cell*. 2000;103(7):1143-54.
35. Pioletti M, Schlunzen F, Harms J, Zarivach R, Gluhmann M, Avila H, et al. Crystal structures of complexes of the small ribosomal subunit with tetracycline, edeine and IF3. *The European Molecular Biology Organization Journal*. 2001;20(8):1829-39.
36. Jenner L, Starosta AL, Terry DS, Mikolajka A, Filonava L, Yusupov M, et al. Structural basis for potent inhibitory activity of the antibiotic tigecycline during protein synthesis. *Proceedings of the National Academy of Sciences of the United States of America*. 2013;110(10):3812-6.
37. Budkevich TV, El'skaya AV, Nierhaus KH. Features of 80S mammalian ribosome and its subunits. *Nucleic Acids Research*. 2008;36(14):4736-44.
38. Ben-Shem A, Garreau de Loubresse N, Melnikov S, Jenner L, Yusupova G, Yusupov M. The structure of the eukaryotic ribosome at 3.0 Å resolution. *Science (New York, NY)*. 2011;334(6062):1524-9.
39. Epe B, Woolley P. The binding of 6-demethylchlortetracycline to 70S, 50S and 30S ribosomal particles: a quantitative study by fluorescence anisotropy. *The European Molecular Biology Organization Journal*. 1984;3(1):121-6.
40. Brown CM, McCaughan KK, Tate WP. Two regions of the Escherichia coli 16S ribosomal RNA are important for decoding stop signals in polypeptide chain termination. *Nucleic Acids Research*. 1993;21(9):2109-15.
41. Chopra I, Hawkey PM, Hinton M. Tetracyclines, molecular and clinical aspects. *The Journal of Antimicrobial Chemotherapy*. 1992;29(3):245-77.
42. Heffron SE, Mui S, Aorora A, Abel K, Bergmann E, Journak F. Molecular complementarity between tetracycline and the GTPase active site of elongation factor Tu. *Acta Crystallographica Section D: Structural Biology*. 2006;62(11):1392-400.
43. Wilson DN. Ribosome-targeting antibiotics and mechanisms of bacterial resistance. *Nature Reviews Microbiology*. 2014;12(1):35-48.
44. Wang Y, Li C, Pielak GJ. Effects of proteins on protein diffusion. *Journal of the American Chemical Society*. 2010;132(27):9392-7.
45. Minton AP. How can biochemical reactions within cells differ from those in test tubes? *Journal of Cell Science*. 2006;119(Pt 14):2863-9.



46. Minton AP. The influence of macromolecular crowding and macromolecular confinement on biochemical reactions in physiological media. *Journal of Biological Chemistry*. 2001;276(14):10577-80.
47. Zimmerman SB, Trach SO. Estimation of macromolecule concentrations and excluded volume effects for the cytoplasm of *Escherichia coli*. *Journal of Molecular Biology*. 1991;222(3):599-620.
48. Chen Z, Zheng KW, Hao YH, Tan Z. Reduced or diminished stabilization of the telomere G-quadruplex and inhibition of telomerase by small chemical ligands under molecular crowding condition. *Journal of the American Chemical Society*. 2009;131(30):10430-8.
49. Fritz BR, Jamil OK, Jewett MC. Implications of macromolecular crowding and reducing conditions for in vitro ribosome construction. *Nucleic Acids Research*. 2015;43(9):4774-84.
50. Miklos AC, Sarkar M, Wang Y, Pielak GJ. Protein crowding tunes protein stability. *Journal of the American Chemical Society*. 2011;133(18):7116-20.
51. Zhou HX. Polymer crowders and protein crowders act similarly on protein folding stability. *Federation of European Biochemical Societies Letters*. 2013;587(5):394-7.
52. Zhou HX, Rivas G, Minton AP. Macromolecular crowding and confinement: biochemical, biophysical, and potential physiological consequences. *Annual Review of Biophysics*. 2008;37:375-97.
53. Miklos AC, Li C, Sharaf NG, Pielak GJ. Volume exclusion and soft interaction effects on protein stability under crowded conditions. *Biochemistry*. 2010;49(33):6984-91.
54. Rajapaksha A, Stanley CB, Todd BA. Effects of macromolecular crowding on the structure of a protein complex: a small-angle scattering study of superoxide dismutase. *Biophysical Journal*. 2015;108(4):967-74.
55. Akabayov SR, Akabayov B, Richardson CC, Wagner G. Molecular crowding enhanced atpase activity of the rna helicase eif4a correlates with compaction of its quaternary structure and association with eIF4G. *Journal of the American Chemical Society*. 2013;135(27):10040-7.
56. Hoffman SJ, Outterson K, Røttingen J-A, Cars O, Clift C, Rizvi Z, et al. An international legal framework to address antimicrobial resistance. *Bulletin World Health Organization* 2015;93(2):66.

57. Infectious Diseases Society of America. The 10 × '20 Initiative: Pursuing a Global Commitment to Develop 10 New Antibacterial Drugs by 2020. *Clinical Infectious Diseases*. 2010;50(8):1081-3.
58. Lewis K. Platforms for antibiotic discovery. *Nature Reviews Drug Discovery*. 2013;12(5):371-87.
59. Payne DJ, Gwynn MN, Holmes DJ, Pompliano DL. Drugs for bad bugs: confronting the challenges of antibacterial discovery. *Nature Reviews Drug Discovery*. 2007;6(1):29-40.
60. Doenhoefer A, Franckenberg S, Wickles S, Berninghausen O, Beckmann R, Wilson DN. Structural basis for TetM-mediated tetracycline resistance. *Proceedings of the National Academy of Sciences of the United States of America*. 2012;109(42):16900-5.
61. Dahl EL, Shock JL, Shenai BR, Gut J, DeRisi JL, Rosenthal PJ. Tetracyclines specifically target the apicoplast of the malaria parasite *Plasmodium falciparum*. *Antimicrobial Agents and Chemotherapy*. 2006;50(9):3124-31.
62. Dibner JJ, Richards JD. Antibiotic growth promoters in agriculture: history and mode of action. *Poultry Science* 2005;84(4):634-43.
63. Huang Y, Zhang L, Tiu L, Wang HH. Characterization of antibiotic resistance in commensal bacteria from an aquaculture ecosystem. *Frontiers in Microbiology*. 2015;6:914.
64. Burke MD. Flexible tetracycline synthesis yields promising antibiotics. *Nature Chemical Biology*. 2009;5(2):77-9.
65. Clark RB, He M, Fyfe C, Lofland D, O'Brien WJ, Plamondon L, et al. 8-Azatetracyclines: synthesis and evaluation of a novel class of tetracycline antibacterial agents. *Journal of Medicinal Chemistry*. 2011;54(5):1511-28.
66. Solomkin JS, Ramesh MK, Cesnauskas G, Novikovs N, Stefanova P, Sutcliffe JA, et al. Phase 2, randomized, double-blind study of the efficacy and safety of two dose regimens of eravacycline versus ertapenem for adult community-acquired complicated intra-abdominal infections. *Antimicrobial Agents and Chemotherapy*. 2014;58(4):1847-54.
67. Aleksandrov A, Simonson T. Binding of tetracyclines to elongation factor Tu, the Tet repressor, and the ribosome: a molecular dynamics simulation study. *Biochemistry*. 2008;47(51):13594-603.

68. Gordon J. Hydrolysis of guanosine 5'-triphosphate associated with binding of aminoacyl transfer ribonucleic acid to ribosomes. *The Journal of Biological Chemistry*. 1969;244(20):5680-6.
69. Lamberti A, Martucci NM, Ruggiero I, Arcari P, Masullo M. Interaction between the antibiotic tetracycline and the elongation factor 1 $\alpha$  from the archaeon *Sulfolobus solfataricus*. *Chemical Biology & Drug Design*. 2011;78(2):260-8.
70. Mesters JR, Potapov AP, de Graaf JM, Kraal B. Synergism between the GTPase activities of EF-Tu•GTP and EF-G•GTP on empty ribosomes: Elongation factors as stimulators of the ribosomal oscillation between two conformations. *Journal of Molecular Biology*. 1994;242(5):644-54.
71. Semenov YP, Makarov EM, Makhno VI, Kirillov SV. Kinetic aspects of tetracycline action on the acceptor (A) site of *Escherichia coli* ribosomes. *Federation of European Biochemical Societies Letters*. 1982;144(1):125-9.
72. Gromadski KB, Wieden H-J, Rodnina MV. Kinetic mechanism of elongation factor Ts-catalyzed nucleotide exchange in elongation factor Tu. *Biochemistry* 2002;41(1):162-9.
73. Dahl LD, Wieden H-J, Rodnina MV, Knudsen CR. The importance of P-loop and domain movements in EF-Tu for guanine nucleotide exchange. *The Journal of Biological Chemistry*. 2006;281(30):21139-46.
74. Leippe DD, Wolf YI, Koonin EV, Aravind L. Classification and evolution of P-loop GTPases and related ATPases. *Journal of Molecular Biology*. 2002;317(1):41-72.
75. Avarsson A. Structure-based sequence alignment of elongation factors Tu and G with related GTPases involved in translation. *Journal of Molecular Evolution*. 1995;41(6):1096-104.
76. Voorhees RM, Schmeing TM, Kelley AC, Ramakrishnan V. The mechanism for activation of GTP hydrolysis on the ribosome. *Science (New York, NY)*. 2010;330(6005):835-8.
77. Mercier E, Girodat D, Wieden H-J. A conserved P-loop anchor limits the structural dynamics that mediate nucleotide dissociation in EF-Tu. *Scientific Reports*. 2015;5:7677.
78. De Laurentiis EI, Mercier E, Wieden H-J. The C-terminal helix of *Pseudomonas aeruginosa* Elongation Factor Ts tunes EF-Tu dynamics to modulate nucleotide exchange. *The Journal of Biological Chemistry*. 2016;291(44):23136-48.

79. Koonin EV, Wolf YI, Aravind L. Protein fold recognition using sequence profiles and its application in structural genomics. *Advances in Protein Chemistry*. 2000;54:245-75.
80. Kawashima T, Berthet-Colominas C, Wulff M, Cusack S, Leberman R. The structure of the *Escherichia coli* EF-Tu•EF-Ts complex at 2.5 Å resolution. *Nature*. 1996;379(6565):511-8.
81. De Laurentiis EI, Mo F, Wieden H-J. Construction of a fully active Cys-less elongation factor Tu: Functional role of conserved cysteine 81. *Biochimica et Biophysica Acta, Proteins and Proteomic*. 2011;1814(5):684-92.
82. Wieden H-J, Mercier E, Gray J, Steed B, Yawney D. A combined molecular dynamics and rapid kinetics approach to Identify conserved three-dimensional communication networks in elongation factor Tu. *Biophysical Journal*. 2010;99(11):3735-43.
83. Gasteiger E, Hoogland C, Gattiker A, Duvaud Se, Wilkins MR, Appel RD, et al. *Protein identification and analysis tools on the Expasy server*: Springer; 2005.
84. Maracci C, Peske F, Dannies E, Pohl C, Rodnina MV. Ribosome-induced tuning of GTP hydrolysis by a translational GTPase. *Proceedings of the National Academy of Sciences of the United States of America*. 2014;111(40):14418-23.
85. Sakellari D, Goodson JM, Kolokotronis A, Konstantinidis A. Concentration of 3 tetracyclines in plasma, gingival crevice fluid and saliva. *Journal of Clinical Periodontology*. 2000;27(1):53-60.
86. Daviter T, Wieden H-J, Rodnina MV. Essential role of histidine 84 in elongation factor Tu for the chemical step of GTP hydrolysis on the ribosome. *Journal of Molecular Biology*. 2003;332(3):689-99.
87. Donner D, Villems R, Liljas A, Kurland CG. Guanosinetriphosphatase activity dependent on elongation factor Tu and ribosomal protein L7/L12. *Proceedings of the National Academy of Sciences of the United States of America*. 1978;75(7):3192-5.
88. Pingoud A, Gast FU, Block W, Peters F. The elongation factor Tu from *Escherichia coli*, aminoacyl-tRNA, and guanosine tetraphosphate form a ternary complex which is bound by programmed ribosomes. *The Journal of Biological Chemistry*. 1983;258(23):14200-5.
89. Nissen P, Kjeldgaard M, Thirup S, Polekhina G, Reshetnikova L, Clark BF, et al. Crystal structure of the ternary complex of Phe-tRNA<sup>Phe</sup>, EF-Tu, and a GTP analog. *Science (New York, NY)*. 1995;270(5241):1464-72.

90. Cayley S, Lewis BA, Guttman HJ, Record Jr MT. Characterization of the cytoplasm of Escherichia coli K-12 as a function of external osmolarity: Implications for protein-DNA interactions in vivo. *Journal of Molecular Biology*. 1991;222(2):281-300.
91. Fuller RS, Kaguni JM, Kornberg A. Enzymatic replication of the origin of the Escherichia coli chromosome. *Proceedings of the National Academy of Sciences of the United States of America*. 1981;78(12):7370-4.
92. Sokolova E, Spruijt E, Hansen MMK, Dubuc E, Groen J, Chokkalingam V, et al. Enhanced transcription rates in membrane-free protocells formed by coacervation of cell lysate. *Proceedings of the National Academy of Sciences*. 2013;110(29):11692-7.
93. Berchtold H, Reshetnikova L, Reiser CO, Schirmer NK, Sprinzl M, Hilgenfeld R. Crystal structure of active elongation factor Tu reveals major domain rearrangements. *Nature*. 1993;365(6442):126-32.
94. Pingoud A, Gast FU, Block W, Peters F. The elongation factor Tu from Escherichia coli, aminoacyl-tRNA, and guanosine tetraphosphate form a ternary complex which is bound by programmed ribosomes. *Journal of Biological Chemistry*. 1983;258(23):14200-5.
95. Thirup SS, Van LB, Nielsen TK, Knudsen CR. Structural outline of the detailed mechanism for elongation factor Ts-mediated guanine nucleotide exchange on elongation factor Tu. *Journal of Structural Biology*. 2015;191(1):10-21.
96. Rivas G, Minton AP. Macromolecular crowding *in vitro*, *in vivo*, and in between. *Trends in Biochemical Sciences*. 2016; 41 (11): 970-98
97. Mukherjee SK, Gautam S, Biswas S, Kundu J, Chowdhury PK. Do Macromolecular Crowding Agents Exert Only an Excluded Volume Effect? A Protein Solvation Study. *The Journal of Physical Chemistry B*. 2015;119(44):14145-56.
98. Qi HW, Nakka P, Chen C, Radhakrishnan ML. The effect of macromolecular crowding on the electrostatic component of barnase-barstar binding: a computational, implicit solvent-based study. *PLoS One*. 2014;9(6):e98618.
99. Christiansen A, Wittung-Stafshede P. Synthetic crowding agent dextran causes excluded volume interactions exclusively to tracer protein apoazurin. *Federation of European Biochemical Societies Letters*. 2014;588(5):811-4.
100. Humphrey W, Dalke A, Schulten K. VMD: visual molecular dynamics. *Journal of Molecular Graphics*. 1996;14(1):33-8, 27-8.

101. Phillips JC, Braun R, Wang W, Gumbart J, Tajkhorshid E, Villa E, et al. Scalable molecular dynamics with NAMD. *Journal of computational chemistry*. 2005;26(16):1781-802.
102. Phillips JC, Braun R, Wang W, Gumbart J, Tajkhorshid E, Villa E, et al. Scalable molecular dynamics with NAMD. *Journal of Computational Chemistry*. 2005;26(16):1781-802.
103. MacKerell Jr AD, Bashford D, Bellott M, Dunbrack Jr RL, Evanseck JD, Field MJ, et al. All-atom empirical potential for molecular modeling and dynamics studies of proteins. *The Journal of Physical Chemistry B*. 1998;102(18):3586-616.
104. Foloppe N, MacKerell Jr AD. All - atom empirical force field for nucleic acids: I. Parameter optimization based on small molecule and condensed phase macromolecular target data. *Journal of Computational Chemistry*. 2000;21(2):86-104.
105. Greer KA, McReynolds MR, Brooks HL, Hoying JB. CARMA: A platform for analyzing microarray datasets that incorporate replicate measures. *BioMed Central Bioinformatics*. 2006;7:149.
106. Wieden H-J, Mercier E, Gray J, Steed B, Yawney D. A combined molecular dynamics and rapid kinetics approach to identify conserved three-dimensional communication networks in elongation factor tu. *Biophysical Journal*. 2010;99(11):3735-43.
107. Spiga E, Abriata LA, Piazza F, Dal Peraro M. Dissecting the effects of concentrated carbohydrate solutions on protein diffusion, hydration, and internal dynamics. *The Journal of Physical Chemistry B*. 2014;118(20):5310-21.
108. King JT, Arthur EJ, Brooks CL, 3rd, Kubarych KJ. Crowding induced collective hydration of biological macromolecules over extended distances. *Journal of the American Chemical Society*. 2014;136(1):188-94.
109. Fasano O, Crechet J-B, Parmeggiani A. Preparation of nucleotide-free elongation factor Tu and its stabilization by the antibiotic kirromycin. *Analytical Biochemistry*. 1982;124(1):53-8.
110. Miyawaki O. Hydration state change of proteins upon unfolding in sugar solutions. *Biochimica et Biophysica Acta*. 2007;1774(7):928-35.
111. Fields PA, Wahlstrand BD, Somero GN. Intrinsic versus extrinsic stabilization of enzymes: the interaction of solutes and temperature on A4-lactate dehydrogenase orthologs from warm-adapted and cold-adapted marine fishes. *European Journal of Biochemistry / Federation of European Biochemical Societies Letters*. 2001;268(16):4497-505.

112. Mikaelsson T, Ådén J, Johansson Lennart BÅ, Wittung-Stafshede P. Direct Observation of Protein Unfolded State Compaction in the Presence of Macromolecular Crowding. *Biophysical journal*. 2013;104(3):694-704.
113. Hong J, Gierasch LM. Macromolecular crowding remodels the energy landscape of a protein by favoring a more compact unfolded state. *Journal of the American Chemical Society*. 2010;132(30):10445-52.
114. Burg MB, Ferraris JD. Intracellular organic osmolytes: function and regulation. *The Journal of Biological Chemistry*. 2008;283(12):7309-13.
115. Phillip Y, Schreiber G. Formation of protein complexes in crowded environments – From in vitro to in vivo. *Federation of European Biochemical Societies Letters*. 2013;587(8):1046-52.
116. Minton AP. Excluded volume as a determinant of macromolecular structure and reactivity. *Biopolymers*. 1981;20(10):2093-120.
117. Klumpp S, Scott M, Pedersen S, Hwa T. Molecular crowding limits translation and cell growth. *Proceedings of the National Academy of Sciences*. 2013;110(42):16754-9.
118. Mika JT, Van den Bogaart G, Veenhoff L, Krasnikov V, Poolman B. Molecular sieving properties of the cytoplasm of *Escherichia coli* and consequences of osmotic stress. *Molecular Microbiology*. 2010;77(1):200-7.
119. Mika JT, Poolman B. Macromolecule diffusion and confinement in prokaryotic cells. *Current Opinion in Biotechnology*. 2011;22(1):117-26.
120. Chai Q, Singh B, Peisker K, Metzendorf N, Ge X, Dasgupta S, et al. Organization of ribosomes and nucleoids in *Escherichia coli* cells during growth and in quiescence. *Journal of Biological Chemistry*. 2014.
121. Brocchieri L, Karlin S. Protein length in eukaryotic and prokaryotic proteomes. *Nucleic Acids Res*. 2005;33(10):3390-400.
122. Dalbow DG, Young R. Synthesis time of beta-galactosidase in *Escherichia coli* B/r as a function of growth rate. *Biochemical Journal*. 1975;150(1):13-20.
123. Lill MA. efficient incorporation of protein flexibility and dynamics into molecular docking simulations. *Biochemistry*. 2011;50(28):6157-69.
124. Aleksandrov A, Simonson T. Molecular mechanics models for tetracycline analogs. *Journal of Computational Chemistry*. 2009;30(2):243-55.

125. Mikaelsson T, Ådén J, Wittung-Stafshede P, Johansson Lennart B-Å. Macromolecular crowding effects on two homologs of ribosomal protein S16: protein-dependent structural changes and local interactions. *Biophysical journal*. 2014;107(2):401-10.